https://www.nonsolmecgroup.com/

The effect of actual porous microstructure on the formation of dynamic necks and adiabatic shear bands

J. A. Rodríguez-Martínez

Acknowledgements

This research has received funding from the European Union's Horizon 2020 research and innovation programme under the ERCEA grant agreement Nº 758056

erc European Research Council
Supporting top researchers from anywhere in the world

PURPOSE

INVESTIGATION OF THE FRAGMENTATION BEHAVIOUR OF METALLIC MATERIALS:

THE ROLE OF GEOMETRIC AND MATERIAL DEFECTS IN PRINTED METALS

RED LEONARDO

Fundación BBVA

GOBIERNO DE ESPAÑA
MINISTERIO DE CIENCIA, INNOVACIÓN Y UNIVERSIDADES

AGENCIA ESTATAL DE INVESTIGACIÓN

MARIE CURIE ACTIONS

Acknowledgements

This research has received funding from the European Union's Horizon 2020 research and innovation programme under the ERCEA grant agreement № 758056

erc European Research Council

Supporting top researchers from anywhere in the world

PURPOSE

CAUTION

WORK

IN PROGRESS

WORK IN PROGRESS

Acknowledgements

NΣM Nonlinear Solid Mechanics Group














SUMMARY

1. **Introduction**
2. **Objective and methodology**
3. **Porosity distribution**
4. **Dynamic necking: formability**
5. **Dynamic shear banding: torsion**
6. **Conclusions**

SUMMARY

1. **Introduction**
2. **Objective and methodology**
3. **Porosity distribution**
4. **Dynamic necking: formability**
5. **Dynamic shear banding: torsion**
6. **Conclusions**

1. Introduction

RESEARCH MOTIVATION: PROTECTION APPLICATIONS

Dynamic failure!

(Undesired) Fragmentation

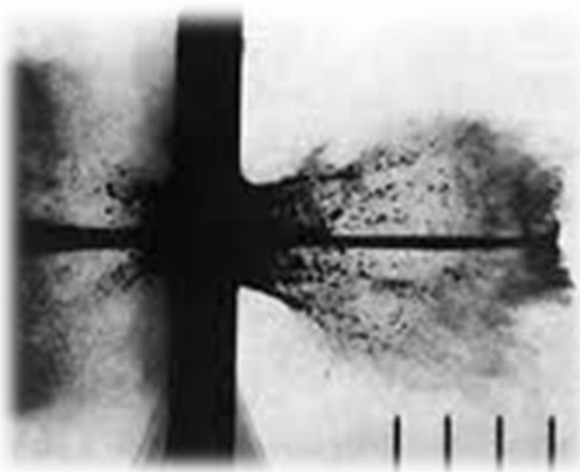

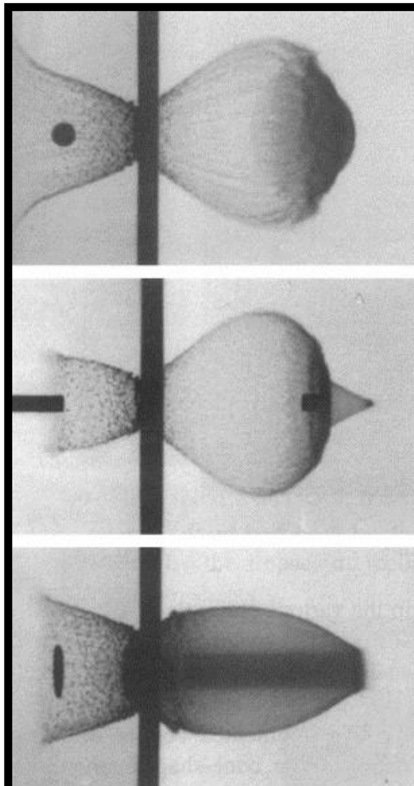

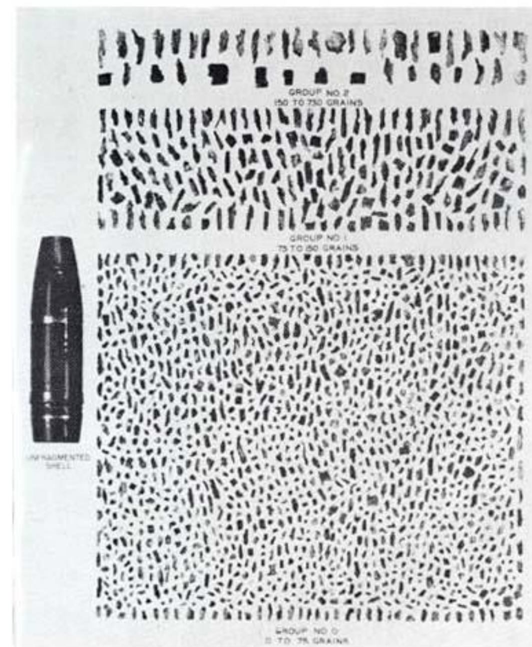

FIGURE 27.—Fragments recovered from a German 75 mm. high explosive shell.

Increase the energy absorption capacity of protective structures!!

1. Introduction

RESEARCH MOTIVATION: METAL WORKING OPERATIONS

Dynamic failure!

(Undesired) Fragmentation

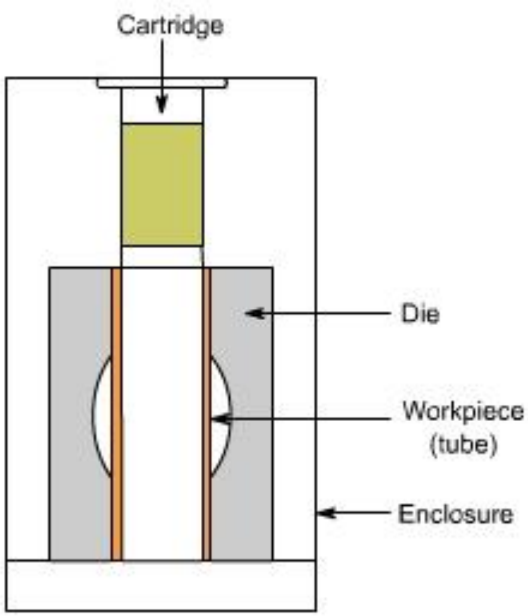

Contact technique of explosive forming
(https://nptel.ac.in/courses/112107144/Metal%20Forming%20&%20Powder%20metallurgy/lecture9/lecture9.htm)

Sequence of underwater explosive forming operations
(https://nptel.ac.in/courses/112107144/Metal%20Forming%20&%20Powder%20metallurgy/lecture9/lecture9.htm)

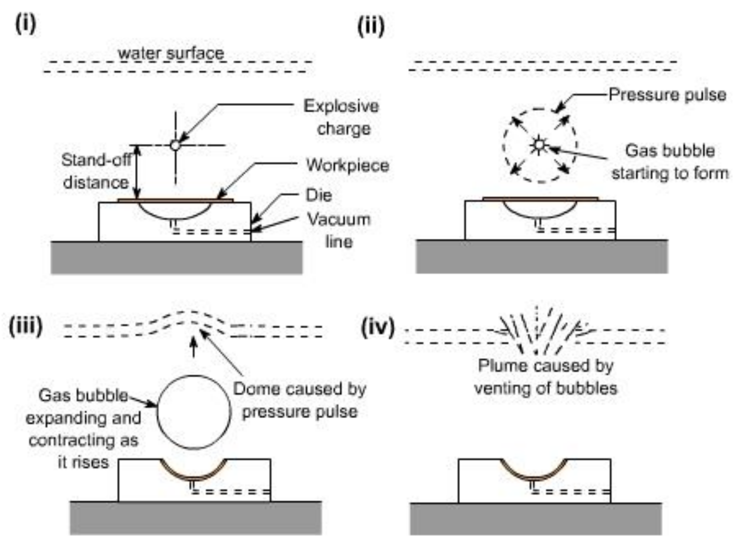

1. Introduction

APPLICATIONS

Dynamic failure!

Fragmentation

What is the influence of ACTUAL MATERIAL POROSITY on multiple flow localization and fragmentation?

ADDITIVELY MANUFACTURED METALS

1. Introduction

APPLICATIONS

Dynamic failure!

Fragmentation

Ductile metallic materials

Multiple flow localization → **Fragmentation**

Shear bands

Necks

1. Introduction

APPLICATIONS

Dynamic failure!

Fragmentation

Ductile metallic materials

Multiple flow localization → Fragmentation

Shear bands

Necks

1. Introduction

APPLICATIONS: laboratory experiment

Dynamic failure!

Fragmentation

Ductile metallic materials

Rapid radial expansion of rings

Zhang and Ravi-Chandar (2006)
University of Texas at Austin

Multiple necking and fragmentation

Uniaxial tension

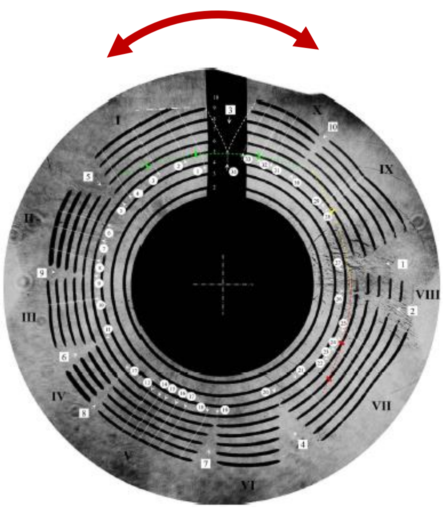

Uniaxial tension

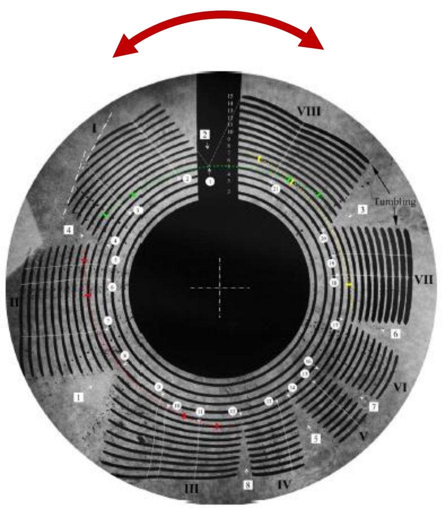

Some necks lead to fracture

Some necks are arrested

1. Introduction

APPLICATIONS: laboratory experiment

Dynamic failure!

Fragmentation

Ductile metallic materials

Rapid radial expansion of rings

Zhang and Ravi-Chandar (2006)
University of Texas at Austin

Multiple necking and fragmentation

Diep et al. 2004

$V_0 = 352$ m/s - $39 \leq N \leq 43$

Zhang and Ravi-Chandar 2006

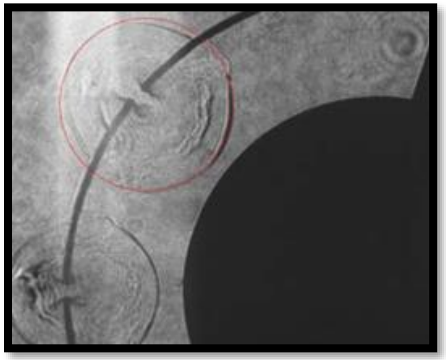

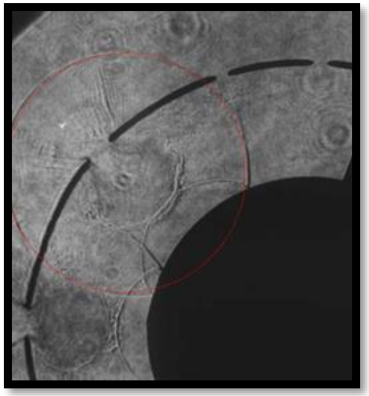

Some necks lead to fracture

1. Introduction

APPLICATIONS: laboratory experiment

Dynamic failure!

Fragmentation

Ductile metallic materials

Rapid radial expansion of rings

Zhang and Ravi-Chandar (2006)
University of Texas at Austin

Multiple necking and fragmentation

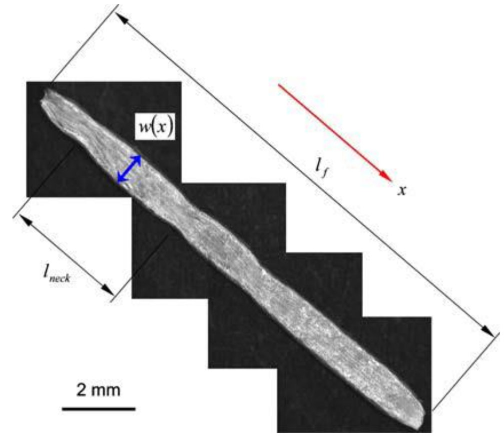

Zhang and Ravi-Chandar 2006

Some necks are arrested

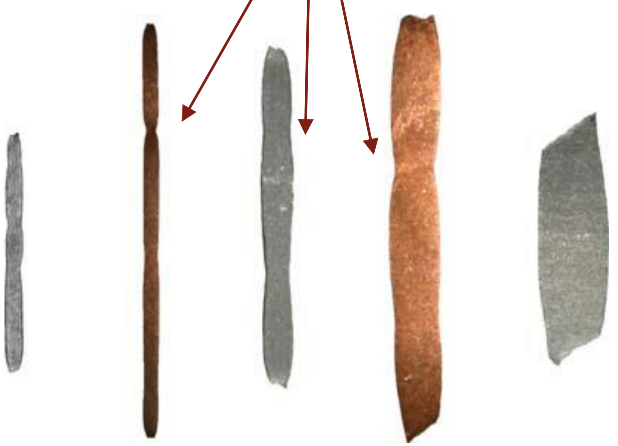

1. Introduction

APPLICATIONS: laboratory experiment

Dynamic failure!

Fragmentation

Ductile metallic materials

Rapid radial expansion of rings

Nieto-Fuentes et al. (2022)
University Carlos III of Madrid

Multiple necking and fragmentation

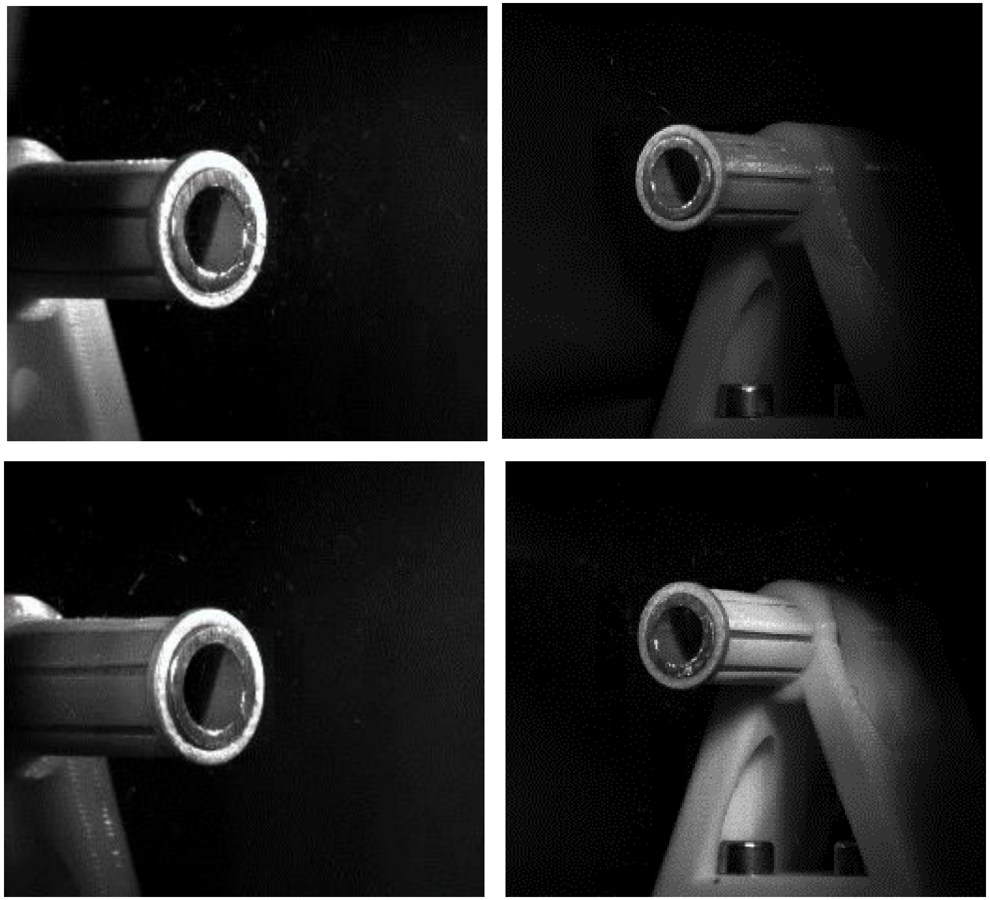

1. Introduction

APPLICATIONS: laboratory experiment

Dynamic failure!

Fragmentation

Ductile metallic materials

Rapid radial expansion of tubes

PhD Thesis Mathieu Xabier (2019)
University of Lorraine

Multiple necking and fragmentation

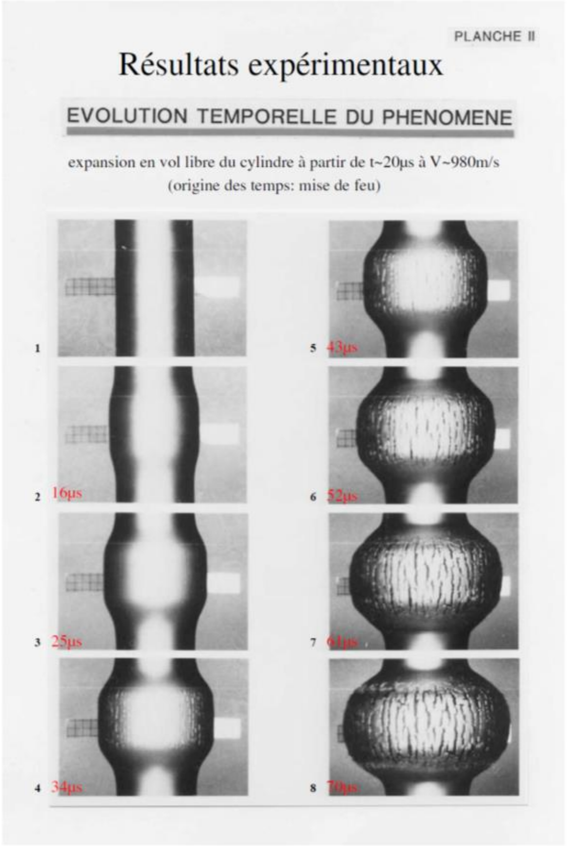

Plane strain

FIGURE 1.13 – *Images réalisées lors de l'expansion par voie détonique du cylindre en acier de l'expérience d'*Olive et al. *(1979) et exploitées par* Jouve *(2010). L'image 2 montre une déformation homogène. À $t = 25$ µs (image 3), les premières localisations suivent les génératrices du cylindre. À $t = 34$ µs (image 4), les strictions sont pleinement développées. Le nombre de strictions par mètre est évalué entre 125 et 150 par mètre par* Jouve *(2010). Les premières ruptures sont apparentes à $t = 52$ µs (image 6).*

1. Introduction

APPLICATIONS: laboratory experiment

Dynamic failure!

Fragmentation

Ductile metallic materials

Rapid radial expansion of hemispherical shells

Mercier et al. (2010)
University of Lorraine

Multiple necking and fragmentation

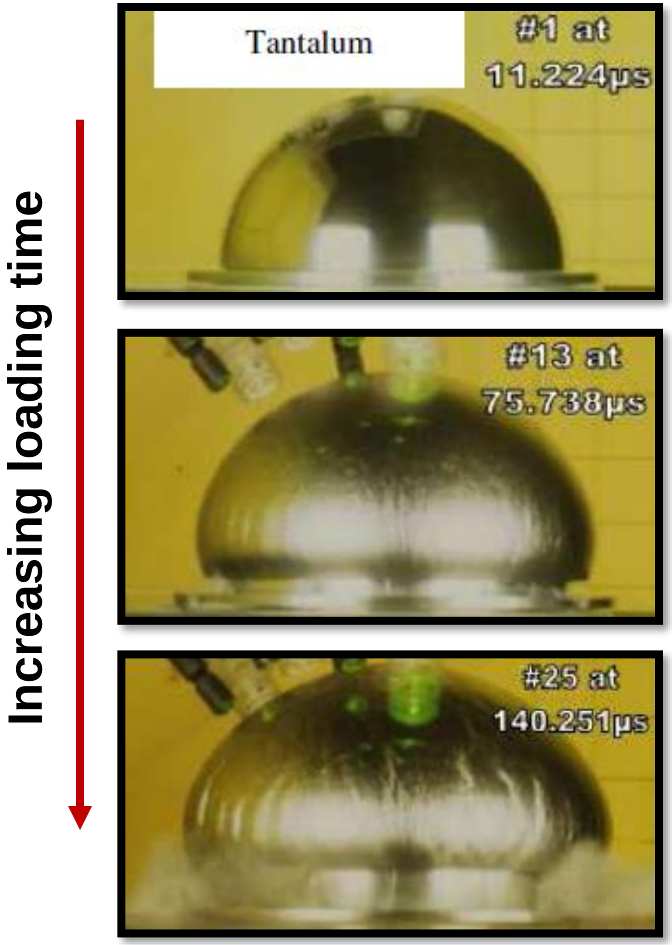

1. Introduction

APPLICATIONS: laboratory experiment

Dynamic failure!

Fragmentation

Ductile metallic materials

Axial penetration of thin-walled tubes

Nieto-Fuentes et al. (2022)
University Carlos III of Madrid

Multiple necking and fragmentation

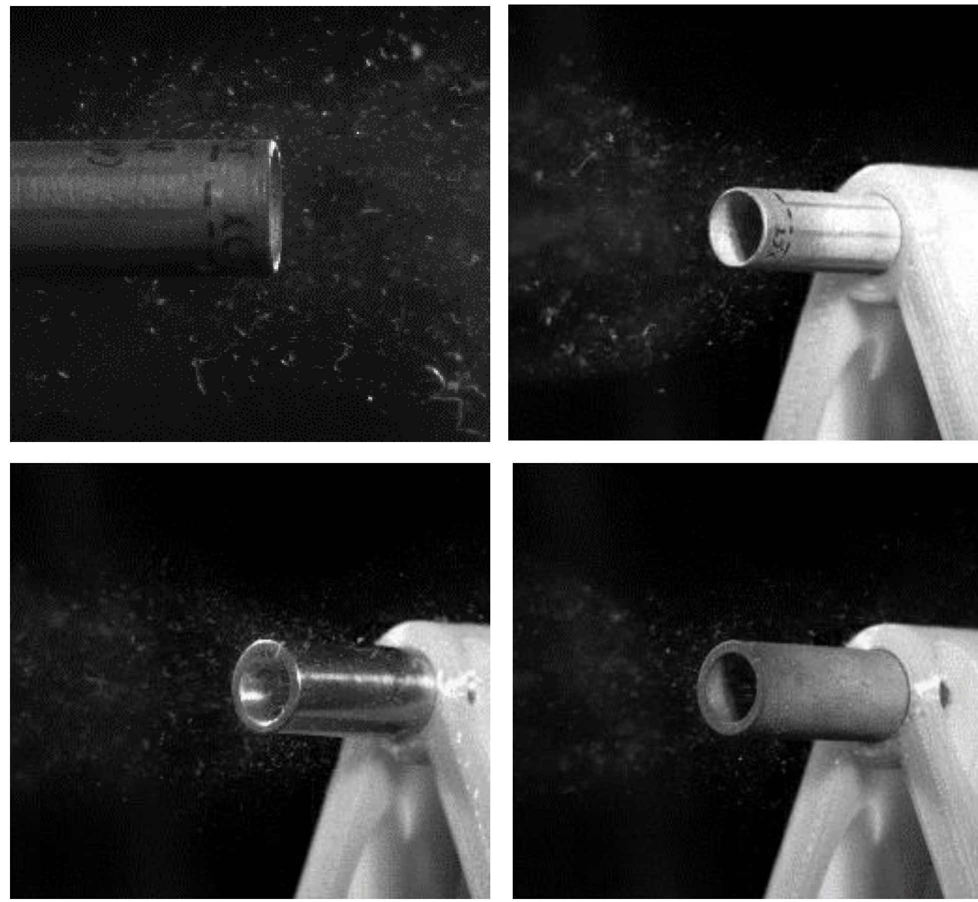

1. Introduction

APPLICATIONS: laboratory experiment

Dynamic failure!

Fragmentation

Ductile metallic materials

Axial penetration of thin-walled tubes

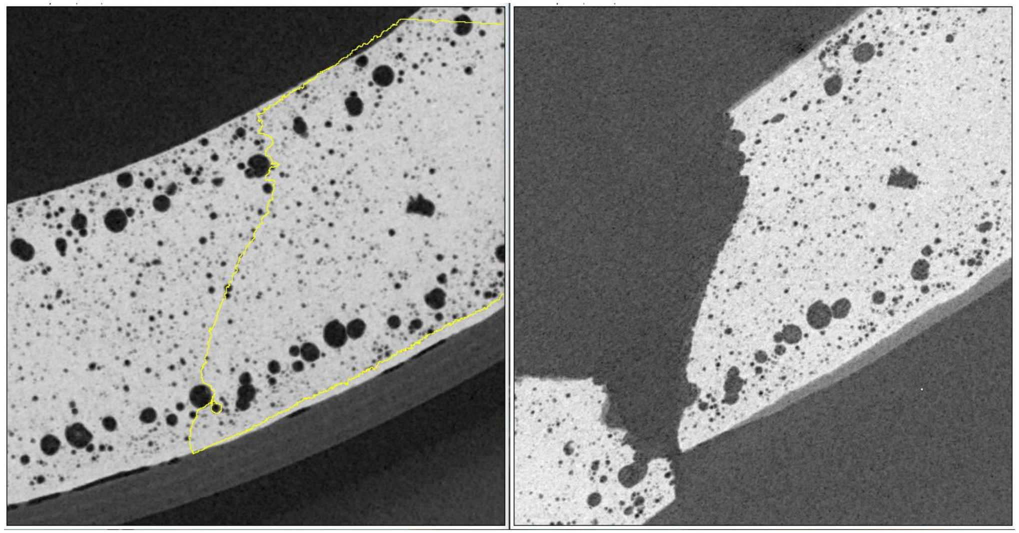

Crack path: The influence of voids

Nieto-Fuentes et al. (2022)
University Carlos III of Madrid

Multiple necking and fragmentation

1. Introduction

APPLICATIONS: laboratory experiment

Dynamic failure!

Fragmentation

Ductile metallic materials

Axial penetration of thin-walled tubes

Nieto-Fuentes et al. (2022)
University Carlos III of Madrid

Multiple necking and fragmentation

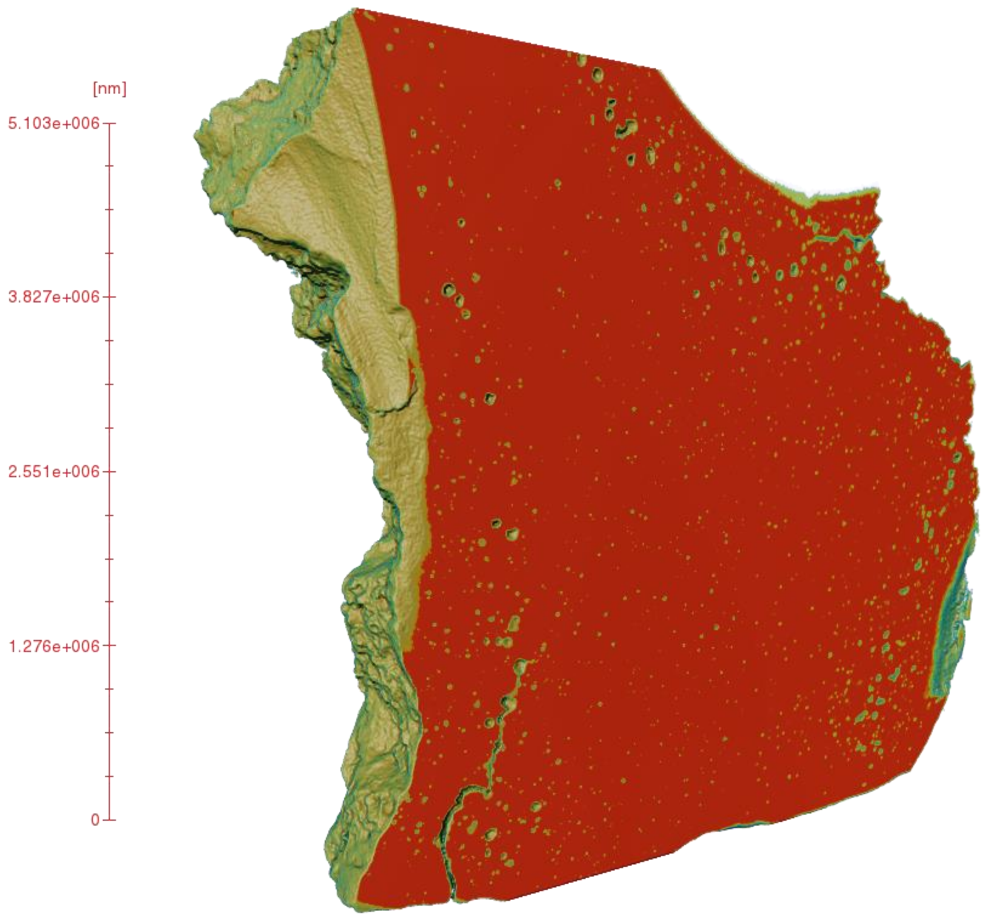

1. Introduction

APPLICATIONS

Dynamic failure!

Fragmentation

Ductile metallic materials

Multiple flow localization → **Fragmentation**

Shear bands

Necks

1. Introduction

APPLICATIONS: laboratory experiment

Dynamic failure!

Ductile metallic materials

Dynamic torsion of thin-walled tubes

Marchand and Duffy (1988)

Specimen after testing

"Forced" shear band

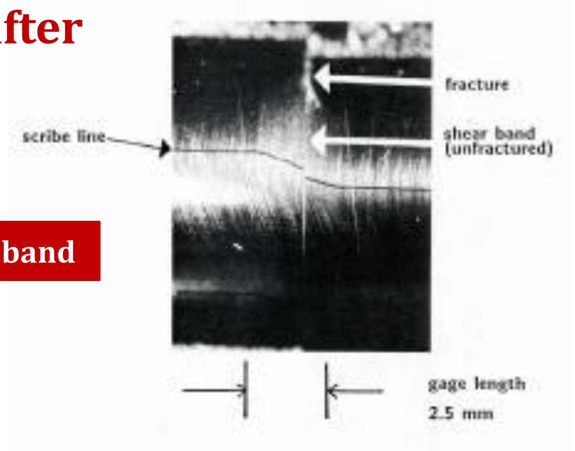

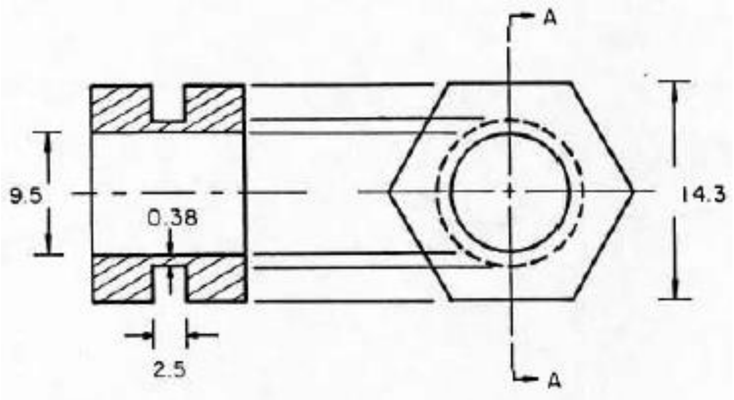

Stages in the formation of a shear band

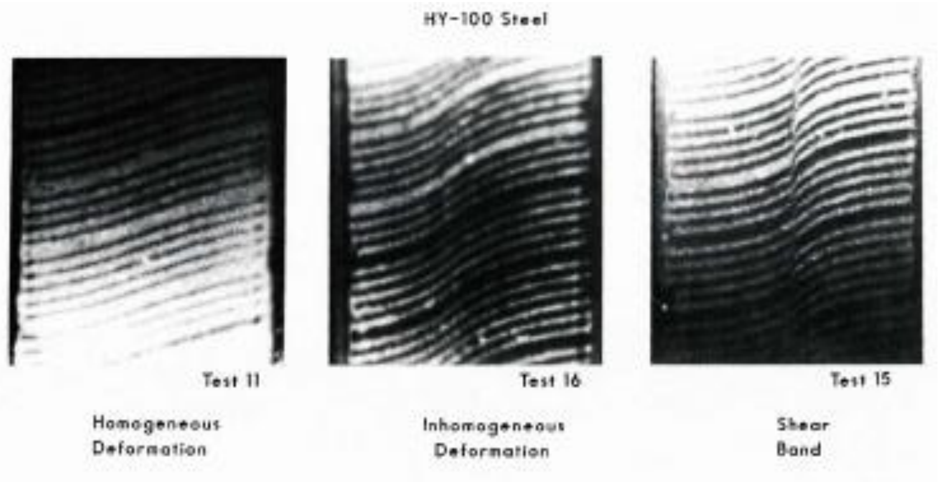

1. Introduction

APPLICATIONS: laboratory experiment

Dynamic failure!

Fragmentation

Ductile metallic materials

Radial collapse of thick-walled tubes

Lovinger et al. (2015)
RAFAEL

Multiple shear banding and fragmentation

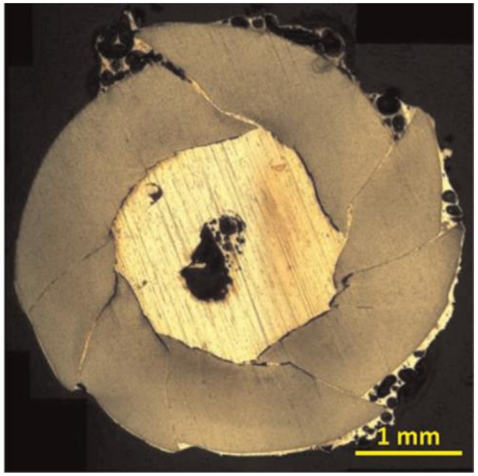

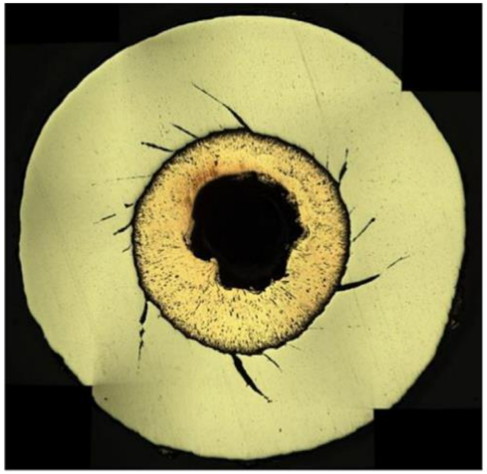

Multiple shear bands develop from the inner radius of the cylinder

1. Introduction

APPLICATIONS: laboratory experiment

Dynamic failure!

Fragmentation

Ductile metallic materials

Radial collapse of thick-walled tubes

Lovinger et al. (2022)
RAFAEL

Multiple shear banding and fragmentation

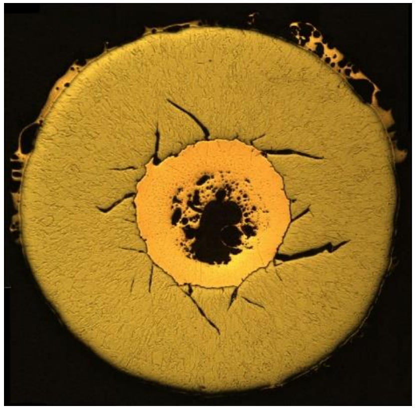

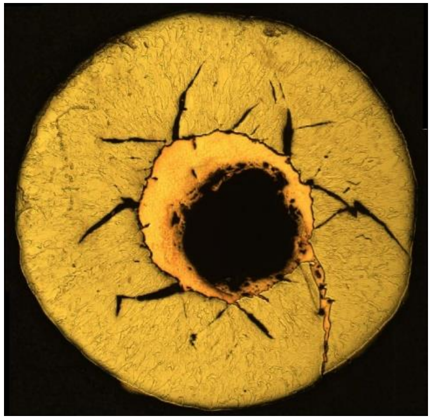

Multiple shear bands develop from the inner radius of the cylinder

1. Introduction

APPLICATIONS: laboratory experiment

Dynamic failure!

Fragmentation

Ductile metallic materials

Radial collapse of thick-walled tubes

Experimental evidence of voids in shear bands

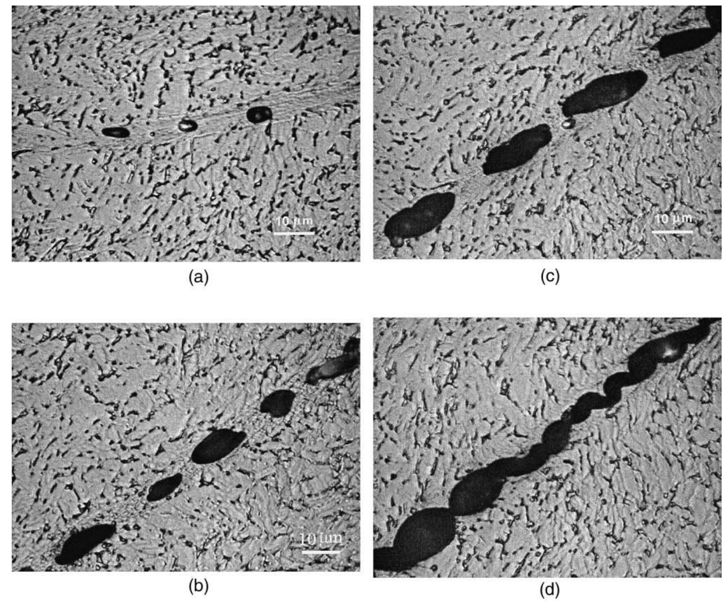

Xue et al. (2002)

Lovinger et al. (2015)

1. Introduction

APPLICATIONS

Dynamic failure!

Fragmentation

Experimental observations

Increasing loading rate increases the number of fragments

Increasing loading rate decreases the number of necks/bands arrested

QUESTION:

What is the specific influence of material defects?

(and the interrelation with inertia?)

1. Introduction

APPLICATIONS

Dynamic failure!

Fragmentation

What is the influence of ACTUAL MATERIAL POROSITY on multiple flow localization and fragmentation?

ADDITIVELY MANUFACTURED METALS

1. Introduction

APPLICATIONS

Dynamic failure!

Fragmentation

APPLICATION TO ADDITIVE MANUFACTURED MATERIALS

Porosity distribution in AlSi10Mg cylindrical specimens

What is the effect on the dynamic energy absorption capacity of the material?

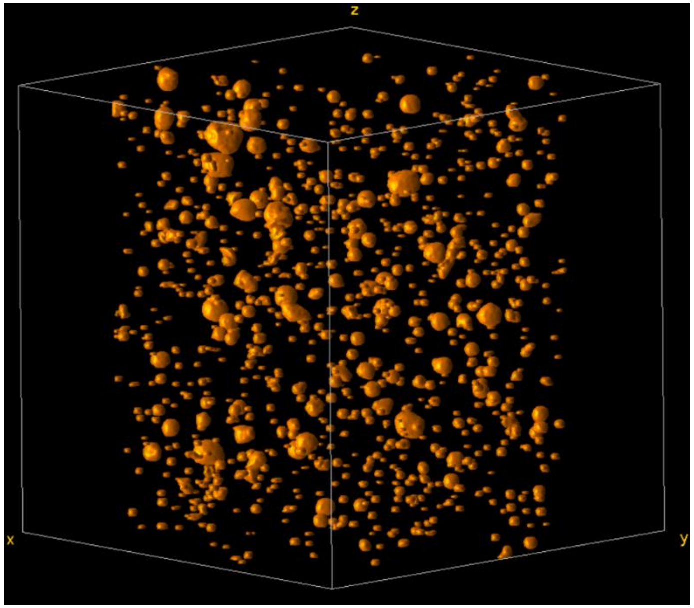

1. Introduction

APPLICATIONS

Dynamic failure!

Fragmentation

NOVELTY

Many papers have investigated the influence of porosity on dynamic localization and fragmentation but ... ALL OF THEM USING HOMOGENIZED GURSON-TYPE CONSTITUTIVE MODELS TO DESCRIBE THE MATERIAL BEHAVIOUR

↓

SPATIAL AND SIZE DISTRIBUTION OF ACTUAL VOIDS

1. Introduction

MODELLING POROUS METALS

Dynamic failure!

Fragmentation

Modelling metallic porous metals

Homogenization: Gurson (1977)

Material displays **periodic porous microstructure** with **spherical voids** and **matrix** described by the **isotropic** yield criterion of von Mises (1928)

THIS IS THE MATERIAL!

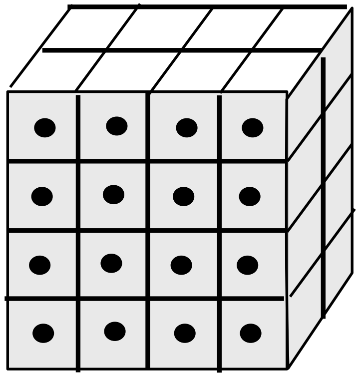

1. Introduction

MODELLING POROUS METALS

Dynamic failure!

Fragmentation

Modelling metallic porous metals

Homogenization: Gurson (1977)

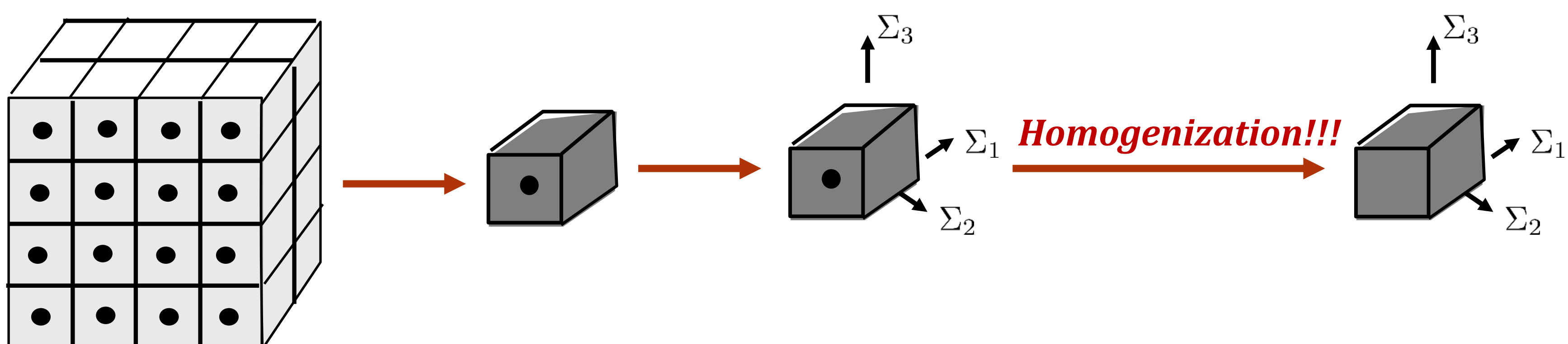

Periodic boundary conditions

*Structure (**macro-scale**)* → *Unit cell (**meso-scale**)*

1. Introduction

MODELLING POROUS METALS

Dynamic failure!

Fragmentation

Modelling metallic porous metals

Homogenization: Gurson (1977)

Homogenization!!! → ***No information on voids size distribution***

$$\Phi\left(\Sigma_h, \Sigma_e, \bar{\sigma}, f\right) = \left(\frac{\Sigma_e}{\bar{\sigma}}\right)^2 + 2q_1 f \cosh\left(\frac{3q_2\Sigma_h}{2\bar{\sigma}}\right) - 1 - \left(q_1 f\right)^2$$

Porosity:
single internal state variable

SUMMARY

1. **Introduction**
2. **Objective and methodology**
3. **Porosity distribution**
4. **Dynamic necking: formability**
5. **Dynamic shear banding: torsion**
6. **Conclusions**

SUMMARY

1. Introduction
2. **Objective and methodology**
3. Porosity distribution
4. Dynamic necking: formability
5. Dynamic shear banding: torsion
6. Conclusions

2. Objective and methodology

Objective

Investigate the effect of ACTUAL porosity (material defects) on the formation of necks and shear bands: application to printed metals

Many papers have investigated using finite elements the role of defects in localization and fragmentation…. None included actual defects!!

The prevailing approach is to include idealized defects decreasing the yield stress of a number of elements, defining random variations of porosity….. Computationally cheap approach which IS NOT representative of actual defects!

Methodology

Finite element simulations with actual distributions of porosity

Own experiments are in process …

SUMMARY

1. **Introduction**
2. **Objective and methodology**
3. **Porosity distribution**
4. **Dynamic necking: formability**
5. **Dynamic shear banding: torsion**
6. **Conclusions**

SUMMARY

1. Introduction
2. Objective and methodology
3. **Porosity distribution**
4. Dynamic necking: formability
5. Dynamic shear banding: torsion
6. Conclusions

3. Porosity distribution

X-ray Computed Tomography

12 porous microstructures AlSi10Mg

Cylindrical specimens with diameter and height of 6 mm were **printed by Selective Laser Melting (SLM)**

↓

Aluminium alloy **$AlSi_{10}Mg$**, stainless steel **316L**, titanium alloy **Ti_6Al_4V** and Inconel **718L**

DIFFERENT PRINTING DIRECTIONS AND RESIDUAL POROSITIES

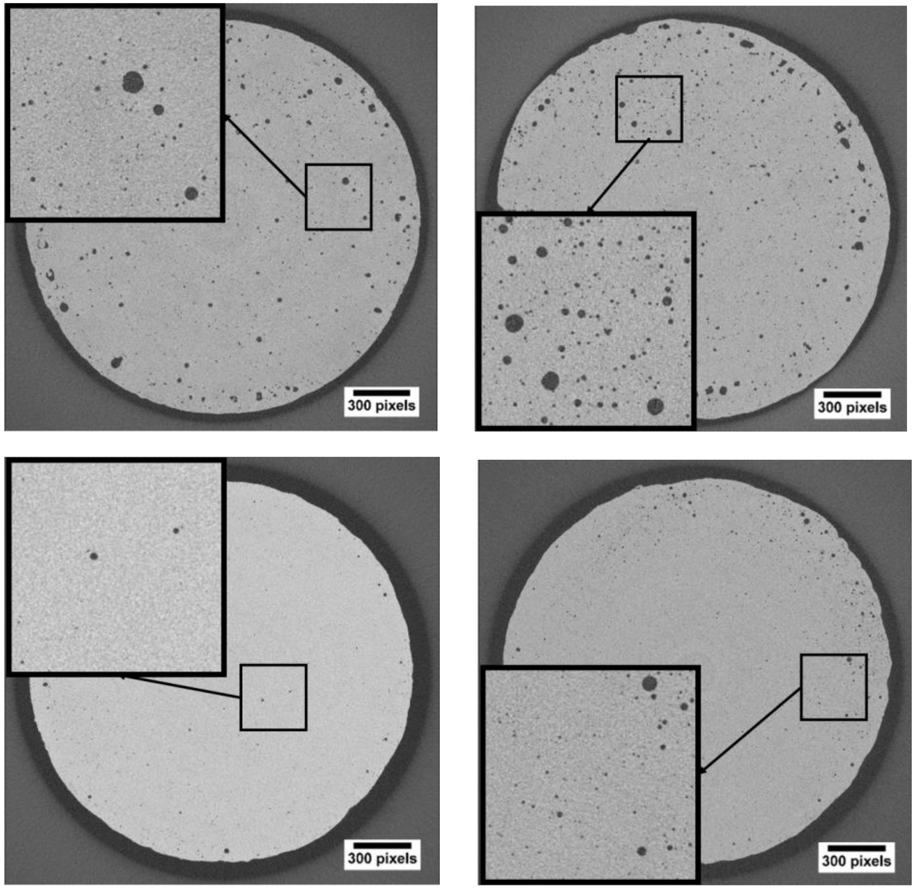

3. Porosity distribution

X-ray Computed Tomography

12 porous microstructures AlSi10Mg

Cylindrical specimens with diameter and height of 6 mm were **printed by Selective Laser Melting (SLM)**

↓

Aluminium alloy **$AlSi_{10}Mg$**, stainless steel **316L**, titanium alloy **Ti_6Al_4V** and Inconel **718L**

DIFFERENT PRINTING DIRECTIONS AND RESIDUAL POROSITIES

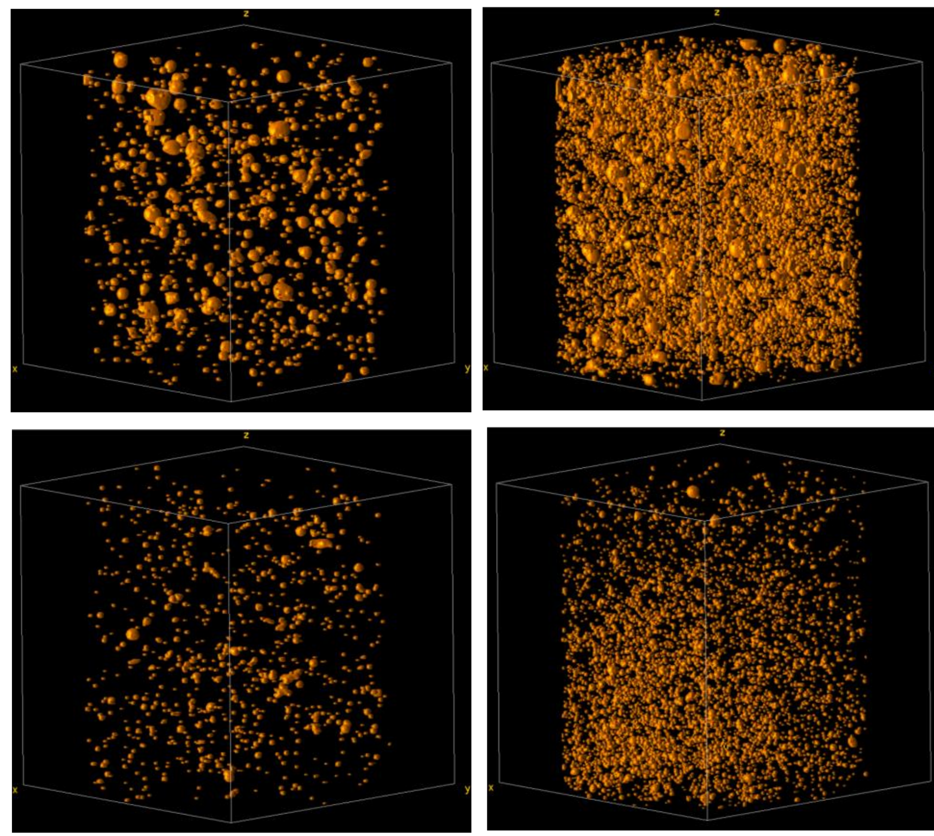

3. Porosity distribution

X-ray Computed Tomography

12 porous microstructures AlSi10Mg

Cylindrical specimens with diameter and height of 6 mm were **printed by Selective Laser Melting (SLM)**

↓

Aluminium alloy **$AlSi_{10}Mg$**, stainless steel **316L**, titanium alloy **Ti_6Al_4V** and Inconel **718L**

DIFFERENT PRINTING DIRECTIONS AND RESIDUAL POROSITIES

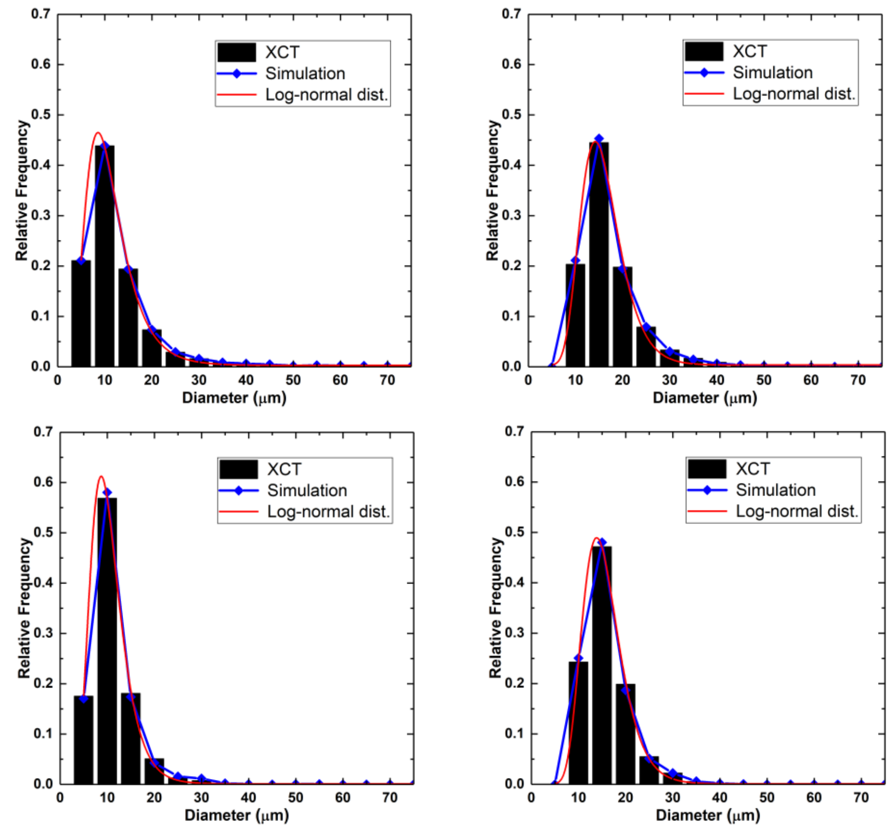

3. Porosity distribution

X-ray Computed Tomography

12 porous microstructures

Log-Normal statistical distribution

	Al3Z	Al3XY	Al0.5Z	Al0.5XY	SS5Z	SS5XY	SS0.5Z	SS0.5XY	Ti0.5Z	Ti0.5XY	INC1Z	INC1XY
VF (%)	1.15	2.17	0.13	0.14	0.0290	0.0025	0.0007	0.0026	0.0033	0.0013	0.1363	0.0203
No. of voids	2500	5985	962	810	18	17	4	38	18	5	147	390
d_{max} (μm)	107	110.53	58.5	41.24	100	41.4	25.9	29.4	31.44	26.93	78.93	45.52
d_{min} (μm)	8.02	8.00	8.1	8.01	7.44	7.40	8.06	8.01	7.44	8.27	7.45	6.36
μ (μm)	11.31	15.98	10.50	15.54	18.45	11.21	11.23	6.83	14.30	17.30	16.58	6.41
dev (μm)	5.03	4.57	3.81	4.37	9.85	5.13	5.04	6.70	9.31	5.03	7.71	4.56

Aluminium alloy **$AlSi_{10}Mg$**, stainless steel **316L**, titanium alloy **Ti_6Al_4V** and Inconel **718L**

DIFFERENT PRINTING DIRECTIONS AND RESIDUAL POROSITIES

SUMMARY

3. Porosity distribution

X-ray Computed Tomography

SLM Φ6-L6 mm

Material

X-ray
Computed
Tomography
(XCT)

Tomographs

Image
processing

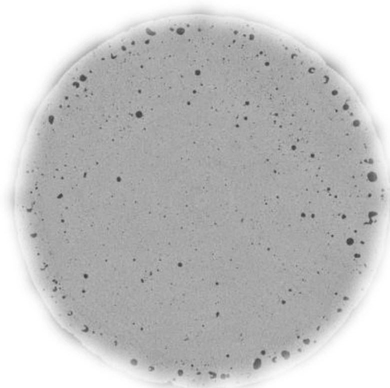

3D reconstruction

ImageJ
(*Schneider et al., 2012*)

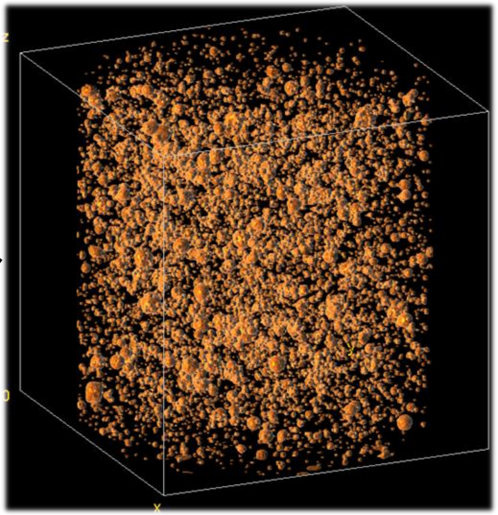

Marvi-Mashhadi et al. (2021)

Diameter of spheres
obtained from XCT

Position of spheres obtained
from *Force Biased Algorithm*
(Bargiel and Moscinski, 1991)

Voids assumed
as spheres

3D model in Abaqus

SUMMARY

1. **Introduction**
2. **Objective and methodology**
3. **Porosity distribution**
4. **Dynamic necking: formability**
5. **Dynamic shear banding: torsion**
6. **Conclusions**

SUMMARY

1. Introduction
2. Objective and methodology
3. Porosity distribution
4. **Dynamic necking: formability**
5. Dynamic shear banding: torsion
6. Conclusions

4. Dynamic necking: formability

Dynamic biaxial stretching of plates

Representative Volume Element:
strip subjected to in-plane loading

The loading condition is determined by the ratio

$$\chi = \frac{\dot{\varepsilon}^0_{yy}}{\dot{\varepsilon}^0_{xx}}$$

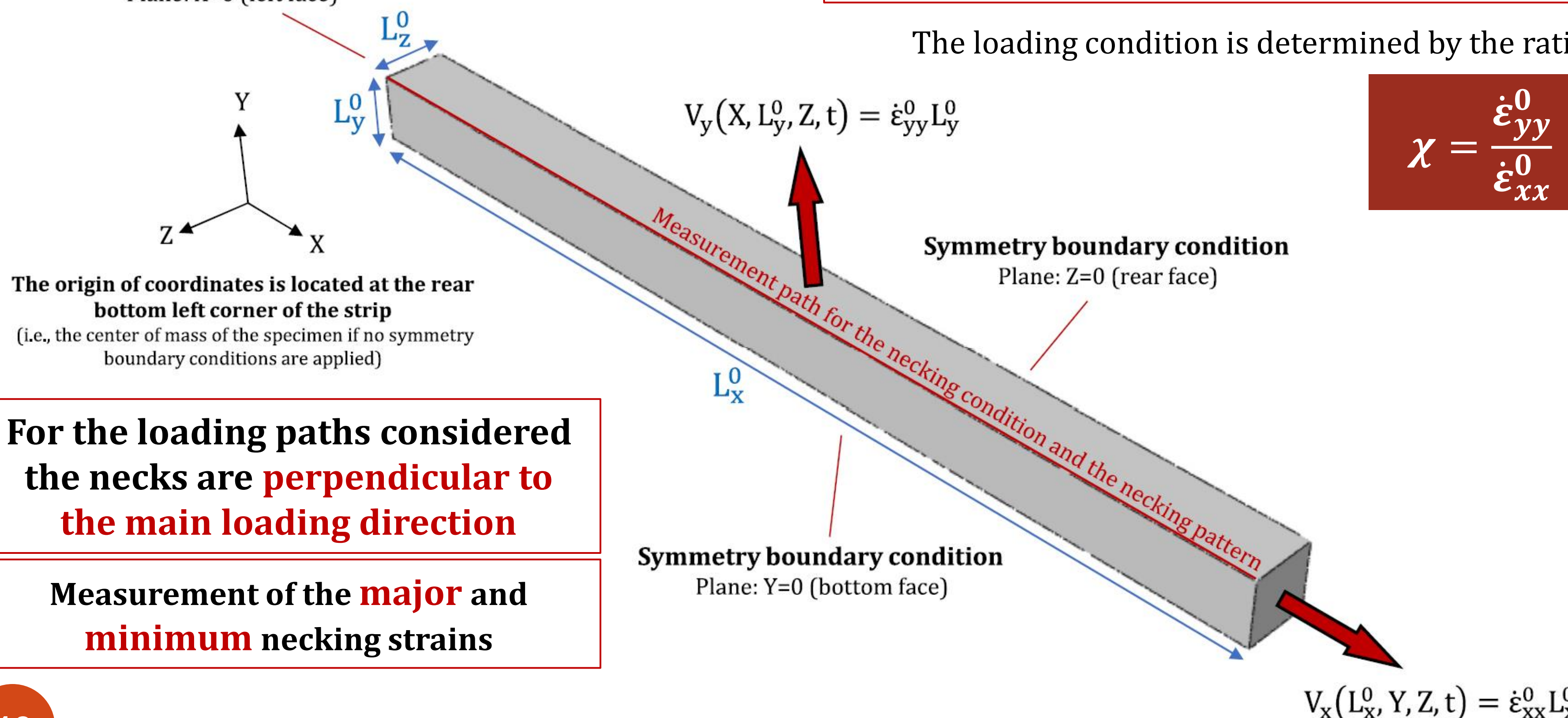

For the loading paths considered the necks are perpendicular to the main loading direction

Measurement of the major and minimum necking strains

4. Dynamic necking: formability

Dynamic biaxial stretching of plates

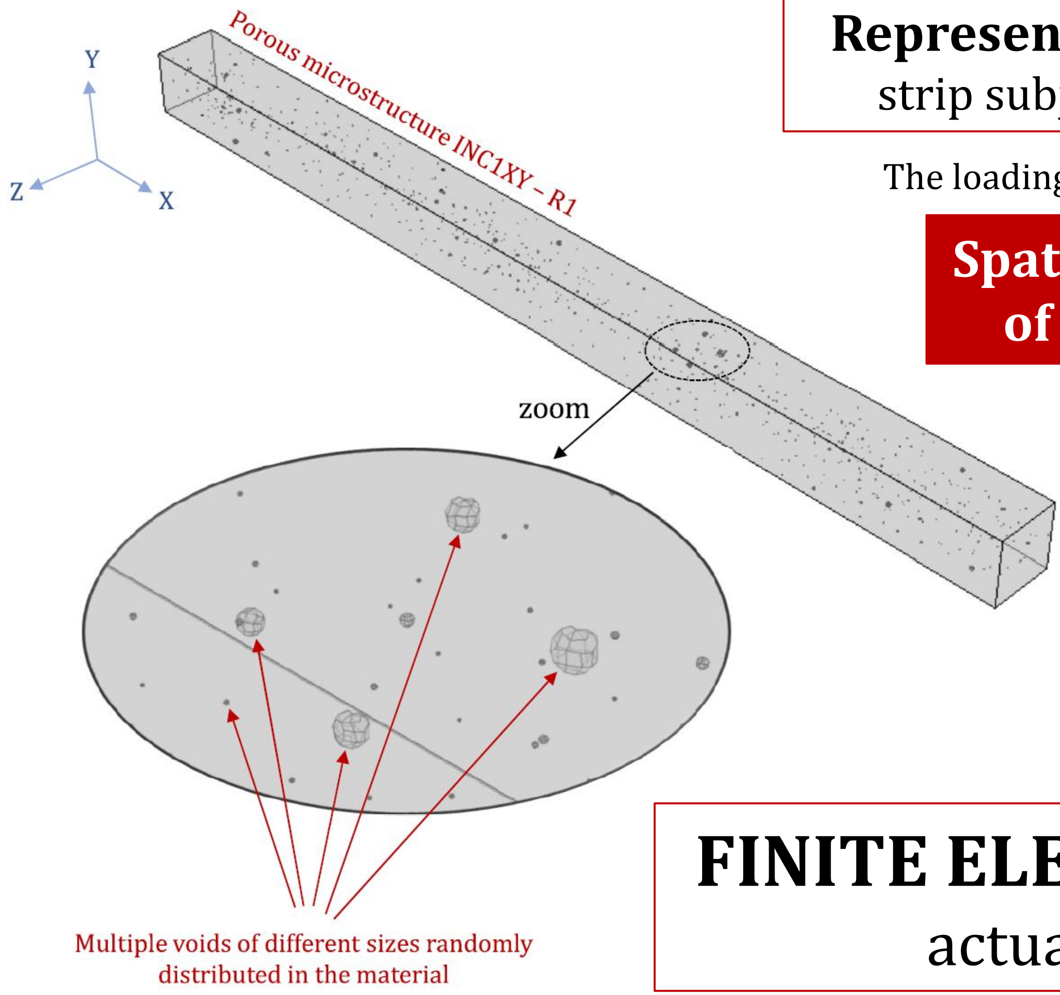

Representative Volume Element: strip subjected to in-plane loading

The loading condition is determined by the ratio

Spatial and size distribution of voids in the specimen

FINITE ELEMENT MODEL:
actual porosity

4. Dynamic necking: formability

Dynamic biaxial stretching of plates

FINITE ELEMENT MODEL:
actual porosity

Representative Volume Element:
strip subjected to in-plane loading

The loading condition is determined by the ratio

Fine mesh to capture the shape of the voids

Large computational cost

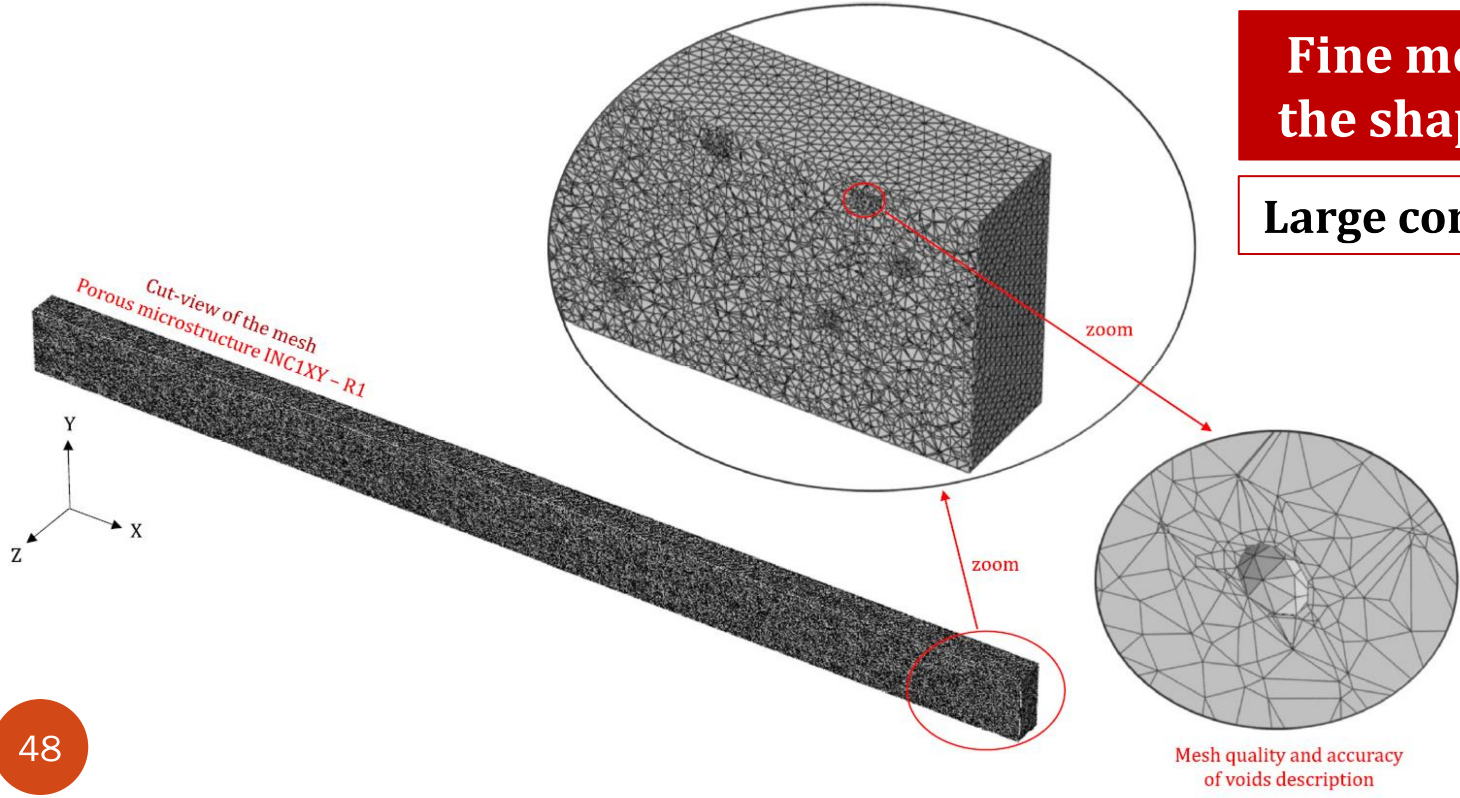

4. Dynamic necking: formability

Dynamic biaxial stretching of plates

FINITE ELEMENT MODEL:
Homogenized porosity

Representative Volume Element:
strip subjected to in-plane loading

Coarse mesh

Small computational cost

The spatial distribution of void volume fraction provides **reasonable** results for the necking strain

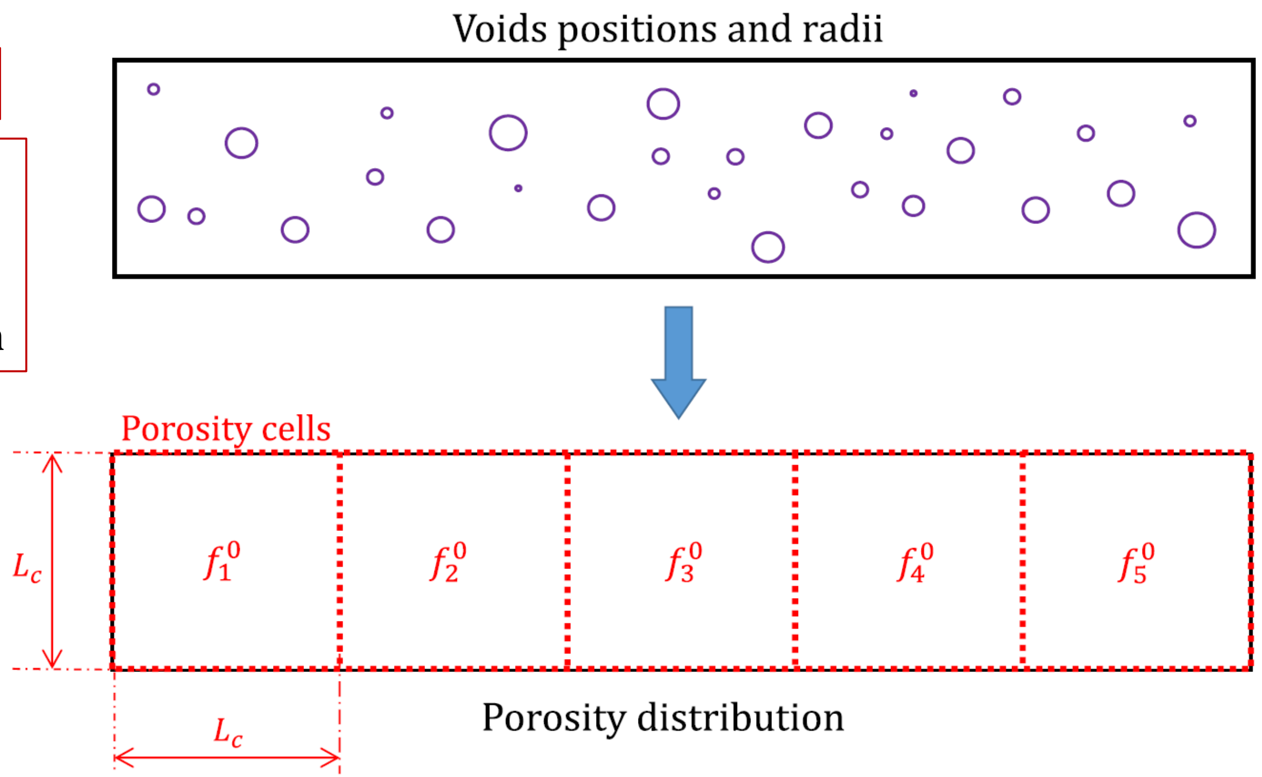

4. Dynamic necking: formability

Mechanical behavior of the material

Linear elasticity and isotropic von Mises plasticity

Yield stress evolution

$$\sigma_Y = \sigma_0 + \sigma_K \left(\bar{\varepsilon}^p\right)^n \left(\frac{\dot{\bar{\varepsilon}}^p}{\dot{\varepsilon}_{ref}}\right)^m \left(\frac{T}{T_{ref}}\right)^{-\mu}$$

Adiabatic conditions of deformation

$$\dot{T} = \beta \frac{\bar{\sigma}\dot{\bar{\varepsilon}}^p}{\rho C_p}$$

Symbol	Property and units	Value
ρ_0	Initial density (kg/m^3)	7740
C_p	Specific heat (J/kg K)	460
E	Young modulus (GPa)	200
ν	Poisson's ratio	0.3
σ_0	Initial yield stress (MPa)	175.67
σ_K	Hardening modulus (MPa)	530.13
n	Strain hardening exponent	0.167
m	Strain rate sensitivity exponent	0.0118
$\dot{\varepsilon}_{ref}$	Reference strain rate (s^{-1})	0.01
μ	Temperature sensitivity exponent	0.51
T_{ref}	Reference temperature (K^{-1})	300
β	Taylor-Quinney coefficient	0.9

WE DO NOT CONSIDER THE SPECIFIC MECHANICAL BEHAVIOUR OF THE PRINTED METALS WHICH ARE ONLY USED TO OBTAIN POROUS MICROSTRUCTURES

4. Dynamic necking: formability

Dynamic biaxial stretching of plates

COMPARISON BETWEEN ACTUAL POROSITY AND HOMOGENIZED POROSITY

Similar necking pattern → **Similar location of necks**

Microstructure: SS5Z – R1

Loading path: $\chi = 0$ – Loading rate: $\dot{\varepsilon}^0_{xx} = 60000\ s^{-1}$

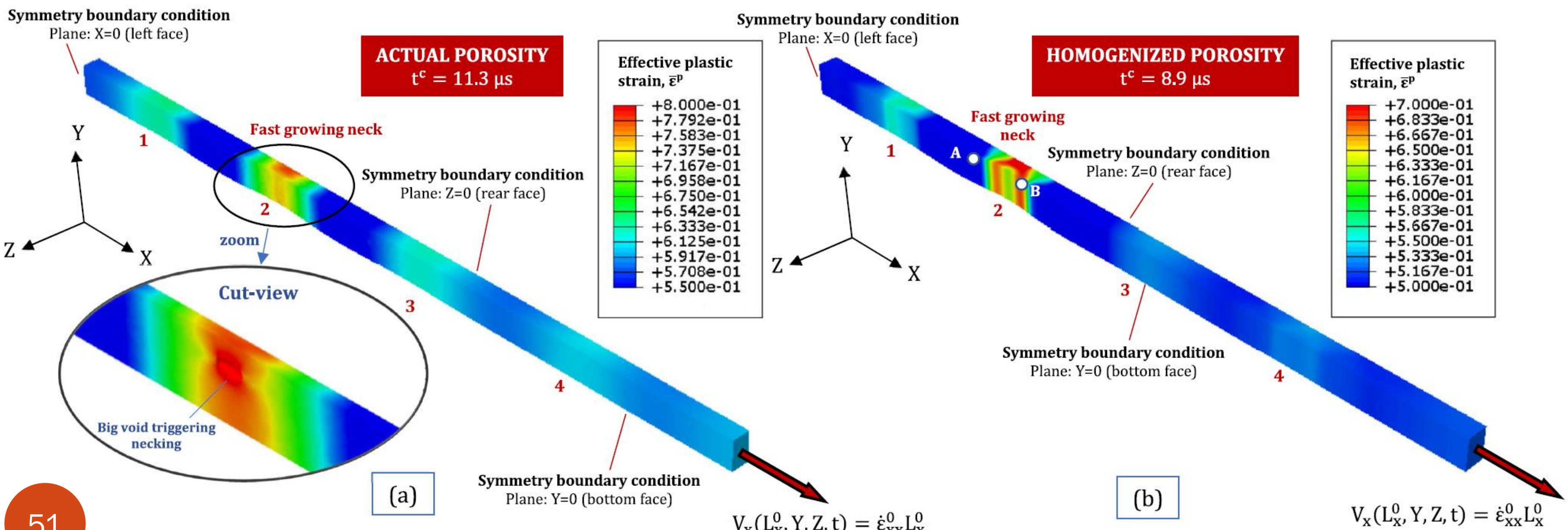

4. Dynamic necking: formability

Dynamic biaxial stretching of plates

COMPARISON BETWEEN ACTUAL POROSITY AND HOMOGENIZED POROSITY

Similar necking pattern → **Similar location of necks**

The locations with large porosity trigger the formation of necks

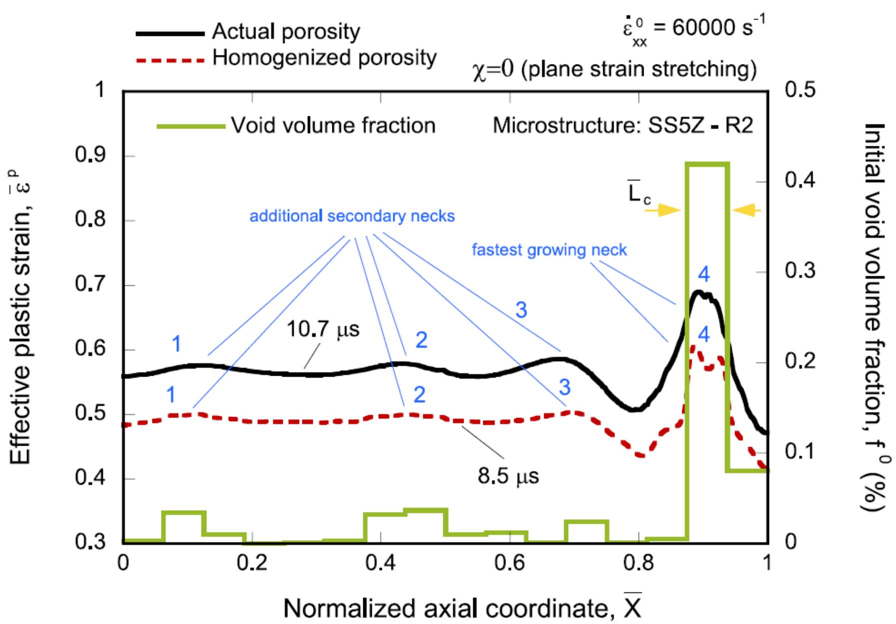

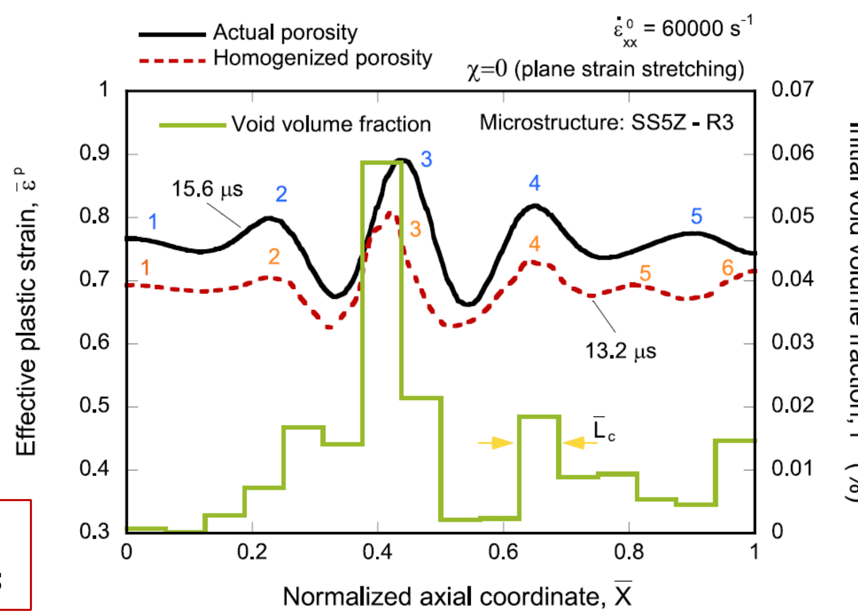

The same general trends for other microstructures, loading paths and strain rates

4. Dynamic necking: formability

Dynamic biaxial stretching of plates

COMPARISON BETWEEN ACTUAL POROSITY AND HOMOGENIZED POROSITY

Evolution of the necking strain with microstructural features

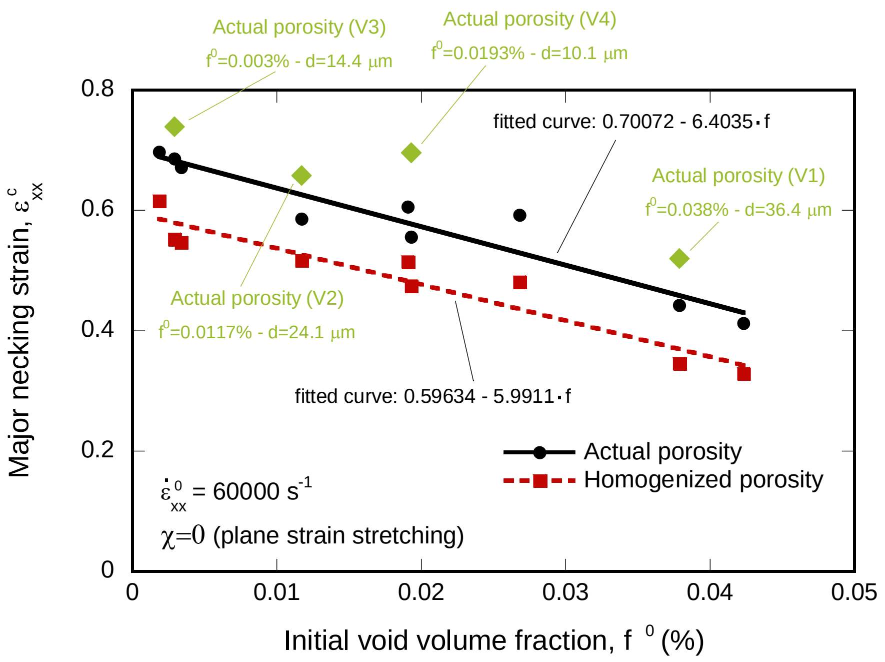

Increasing initial void volume fraction and maximum void diameter lead to a decrease of the necking formability

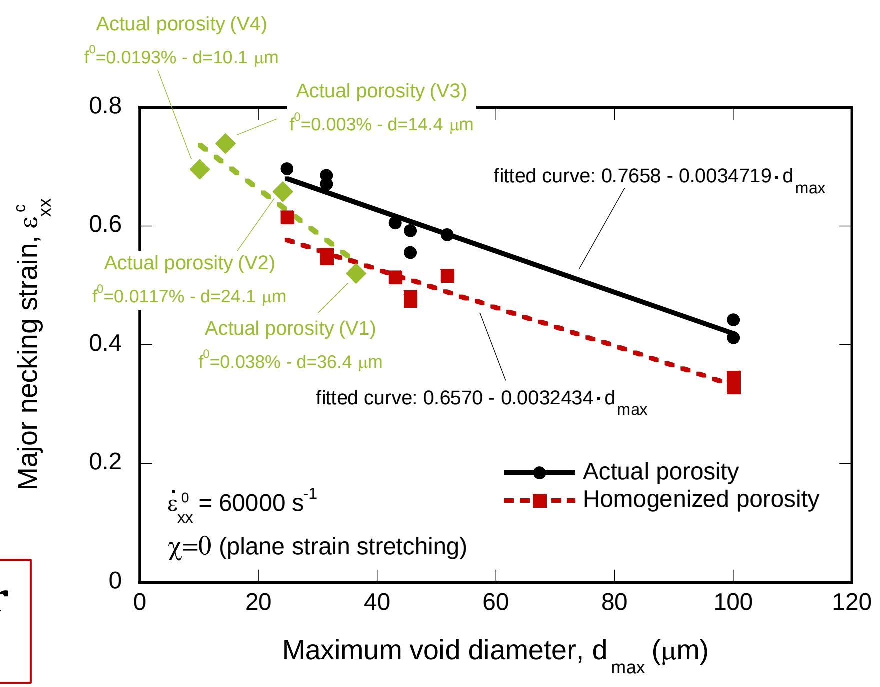

The same general trends for other loading paths and strain rates

4. Dynamic necking: formability

Dynamic biaxial stretching of plates

COMPARISON BETWEEN ACTUAL POROSITY AND HOMOGENIZED POROSITY

Forming limit diagram

The effect of loading path

The effect of inertia

THE DIFFERENCES BETWEEN ACTUAL POROSITY AND HOMOGENIZED POROSITY INCREASE WITH THE STRAIN RATE

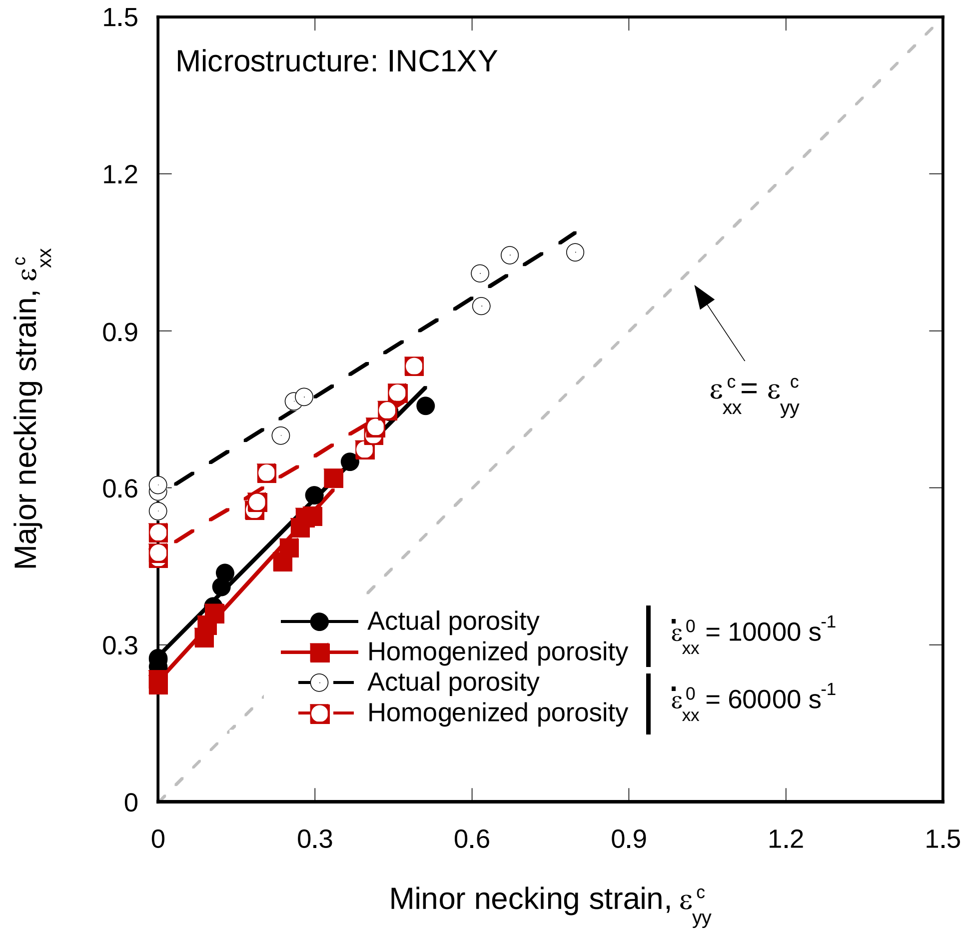

4. Dynamic necking: formability

Dynamic biaxial stretching of plates

*The **homogenized porosity** calculations provide results for the necking strain which are in **qualitative agreement** with the actual porosity simulations, the quantitative differences being generally less that 25%*

***Initial void volume fraction** and **maximum voids size** affect the necking strain, with the initial void volume fraction playing a critical role in the specimen ductility*

*The **number** and the **location** of necks predicted by the homogenized porosity approach and the actual porosity calculations are **very similar** for all loading rates and loading paths investigated*

SUMMARY

1. **Introduction**
2. **Objective and methodology**
3. **Porosity distribution**
4. **Dynamic necking: formability**
5. **Dynamic shear banding: torsion**
6. **Conclusions**

SUMMARY

1. Introduction
2. Objective and methodology
3. Porosity distribution
4. Dynamic necking: formability
5. **Dynamic shear banding: torsion**
6. Conclusions

5. Dynamic shear banding: torsion

Dynamic twisting of thin-walled tube

Representative Volume Element: strip subjected to angular velocity

Fine mesh to capture the shape of the voids

Large computational cost

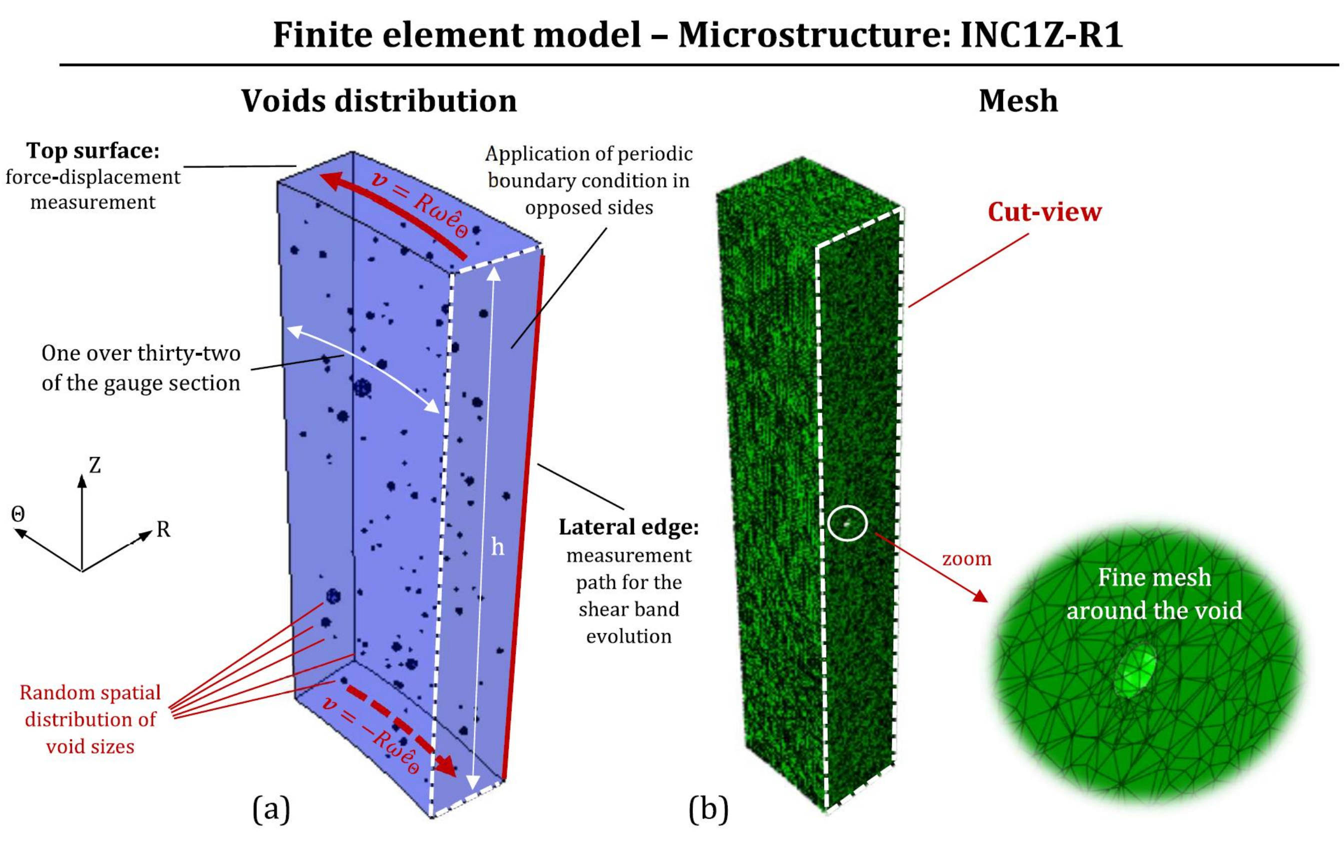

4. Dynamic necking: formability

Mechanical behavior of the material

Linear elasticity and isotropic von Mises plasticity

Yield stress evolution

$$\sigma_Y = \sigma_0 + \sigma_K \left(\bar{\varepsilon}^p\right)^n \left(\frac{\dot{\bar{\varepsilon}}^p}{\dot{\varepsilon}_{ref}}\right)^m \left(\frac{T}{T_{ref}}\right)^{-\mu}$$

Adiabatic conditions of deformation

$$\dot{T} = \beta \frac{\bar{\sigma}\dot{\bar{\varepsilon}}^p}{\rho C_p}$$

Symbol	Property and units	Value
ρ_0	Initial density (kg/m^3)	7740
C_p	Specific heat (J/kg K)	460
E	Young modulus (GPa)	200
ν	Poisson's ratio	0.3
σ_0	Initial yield stress (MPa)	175.67
σ_K	Hardening modulus (MPa)	530.13
n	Strain hardening exponent	0.167
m	Strain rate sensitivity exponent	0.0118
$\dot{\varepsilon}_{ref}$	Reference strain rate (s^{-1})	0.01
μ	Temperature sensitivity exponent	0.51
T_{ref}	Reference temperature (K^{-1})	300
β	Taylor-Quinney coefficient	0.9

WE DO NOT CONSIDER THE SPECIFIC MECHANICAL BEHAVIOUR OF THE PRINTED METALS WHICH ARE ONLY USED TO OBTAIN POROUS MICROSTRUCTURES

5. Dynamic shear banding: torsion

Onset and development of shear band

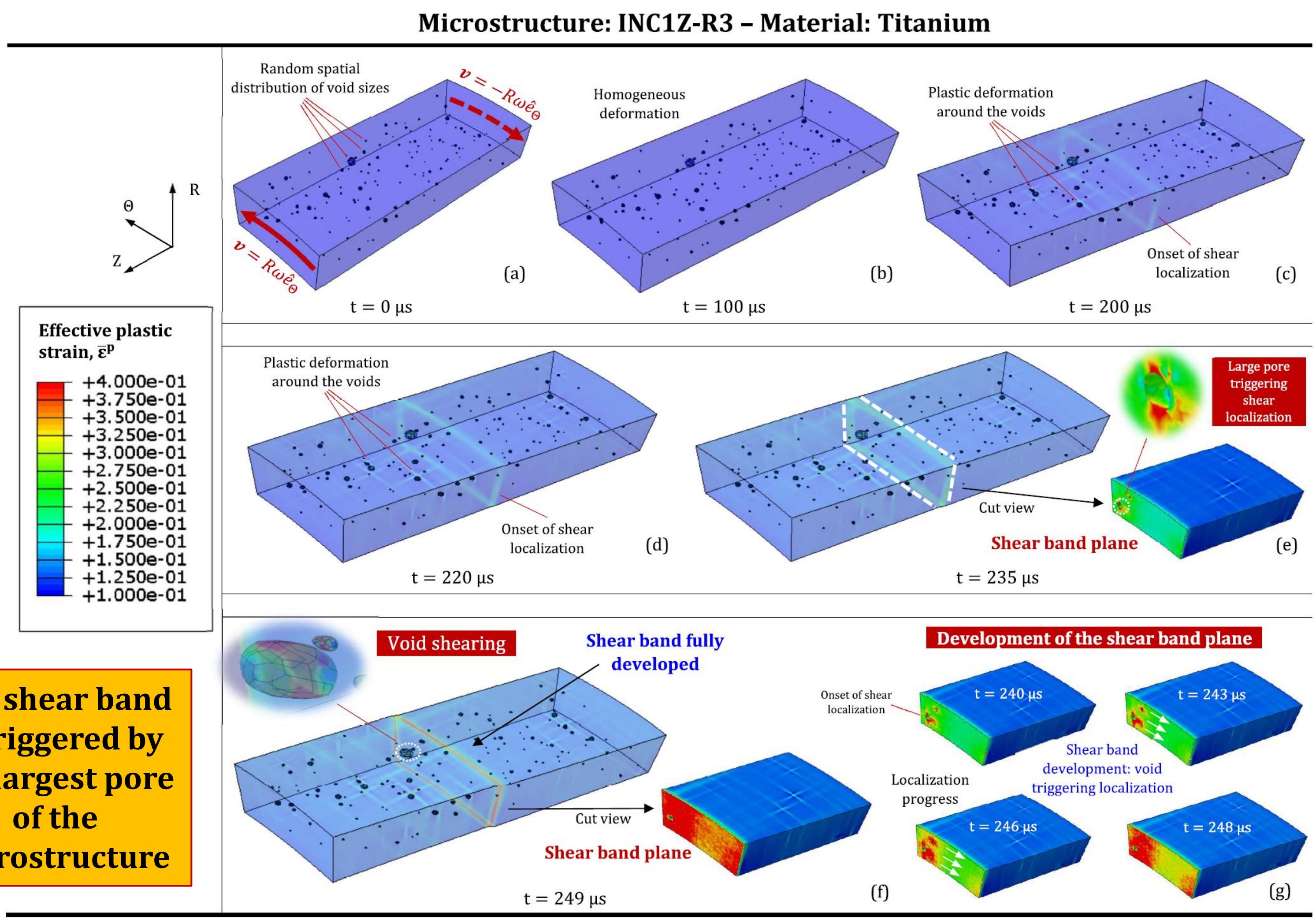

The shear band is triggered by the largest pore of the microstructure

5. Dynamic shear banding: torsion

Comparison with fully dense material

Porosity leading to early shear localization: loss of load carrying capacity

Porous microstructure breaks the symmetry of the problem: shear band incepted by the greatest void of the microstructure

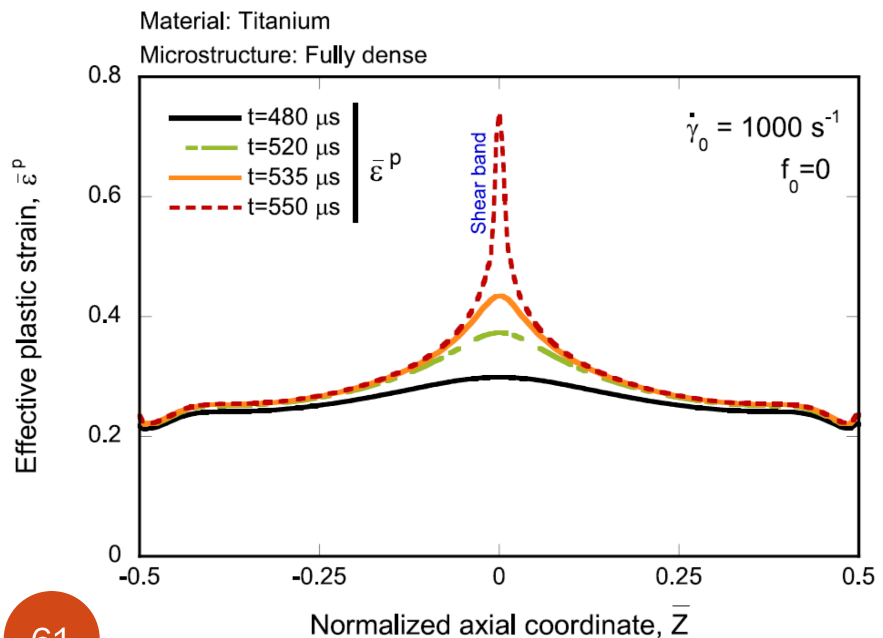

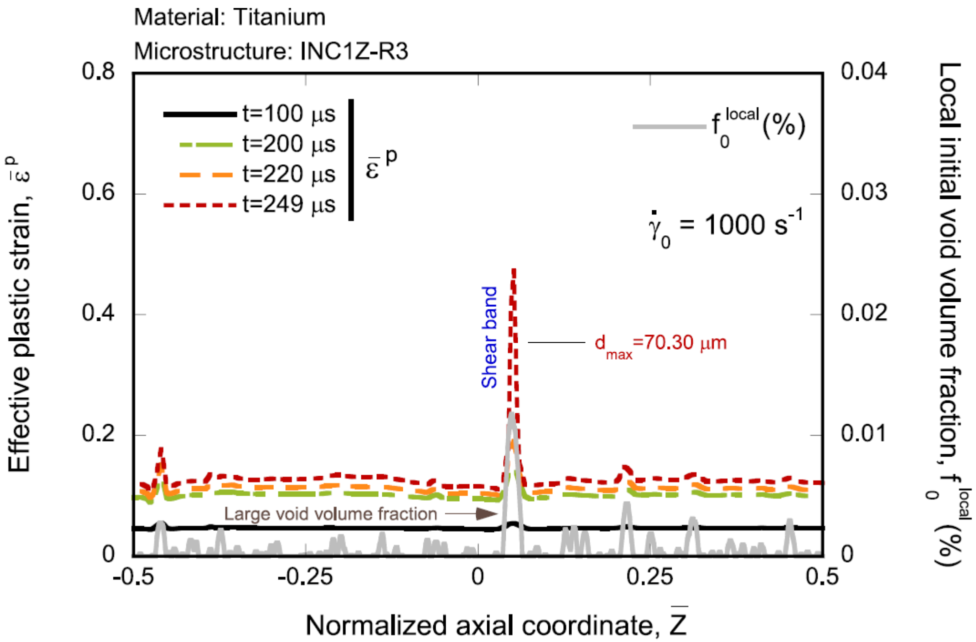

5. Dynamic shear banding: torsion

Comparison with fully dense material

Porosity leading to early shear localization: loss of load carrying capacity

Shear band formation after the maximum force

NO evolution of void volume fraction

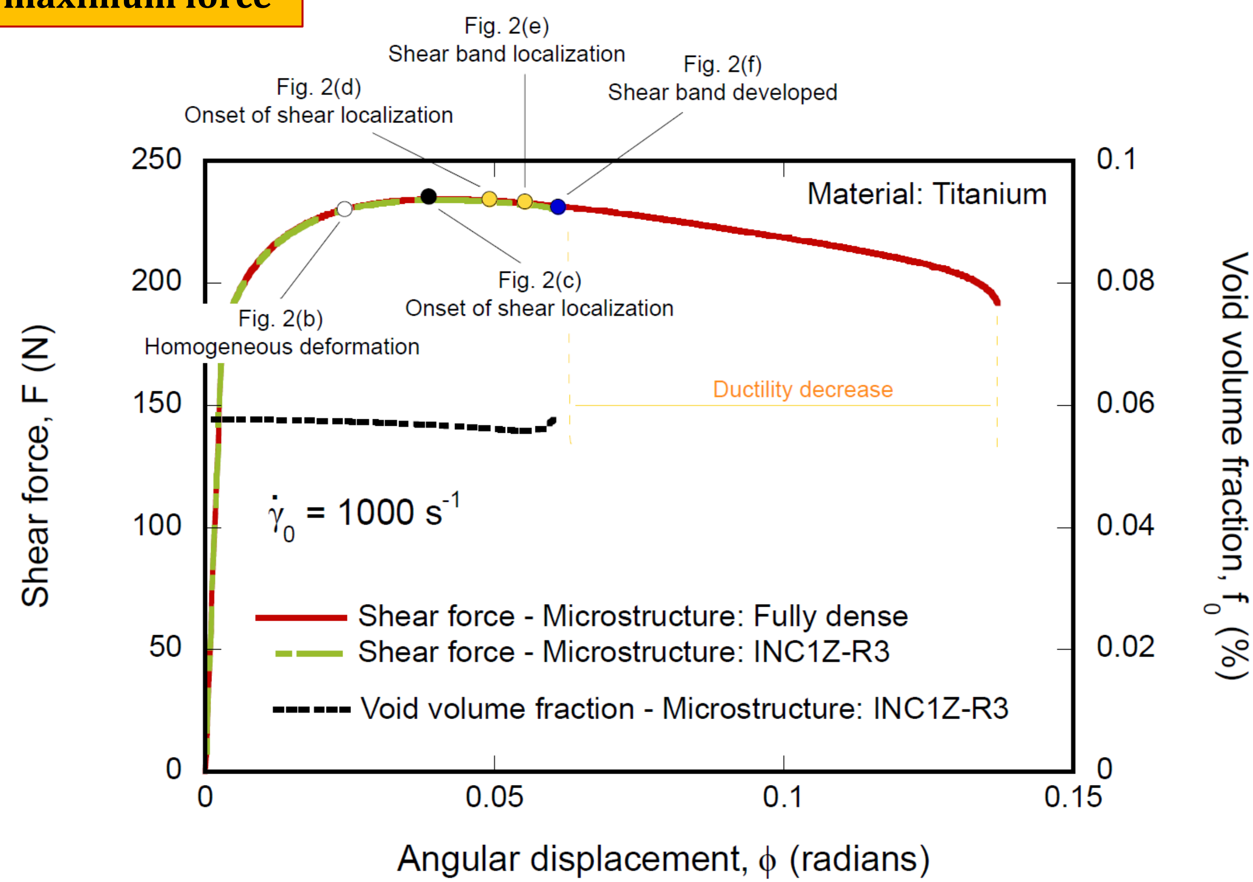

5. Dynamic shear banding: torsion

The effect of porous microstructure

The loss of load carrying capacity depends on the porous microstructure

Shear band formation after the maximum force

What determines the loss of load carrying capacity?

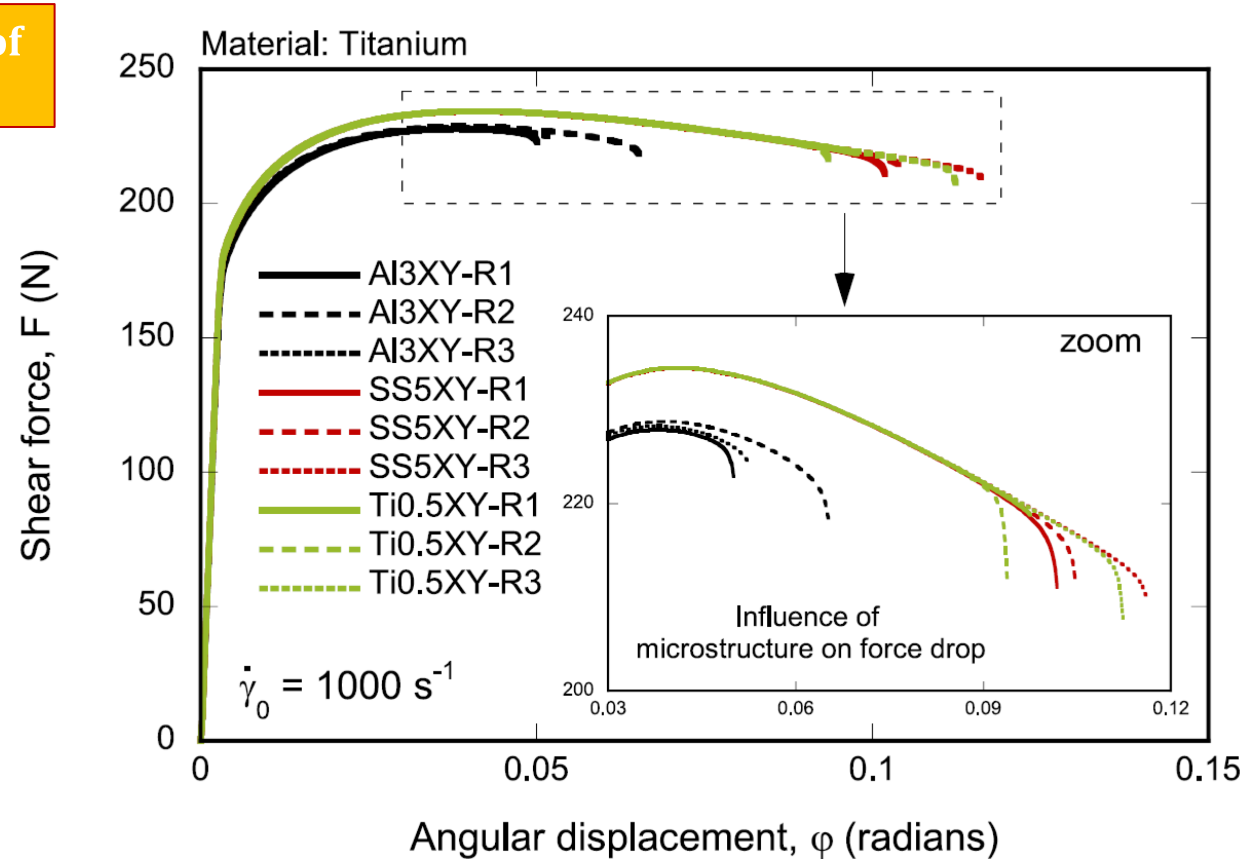

5. Dynamic shear banding: torsion

The effect of porous microstructure

The loss of load carrying capacity depends on the porous microstructure

THE EFFECT OF THE INITIAL VOID VOLUME FRACTION

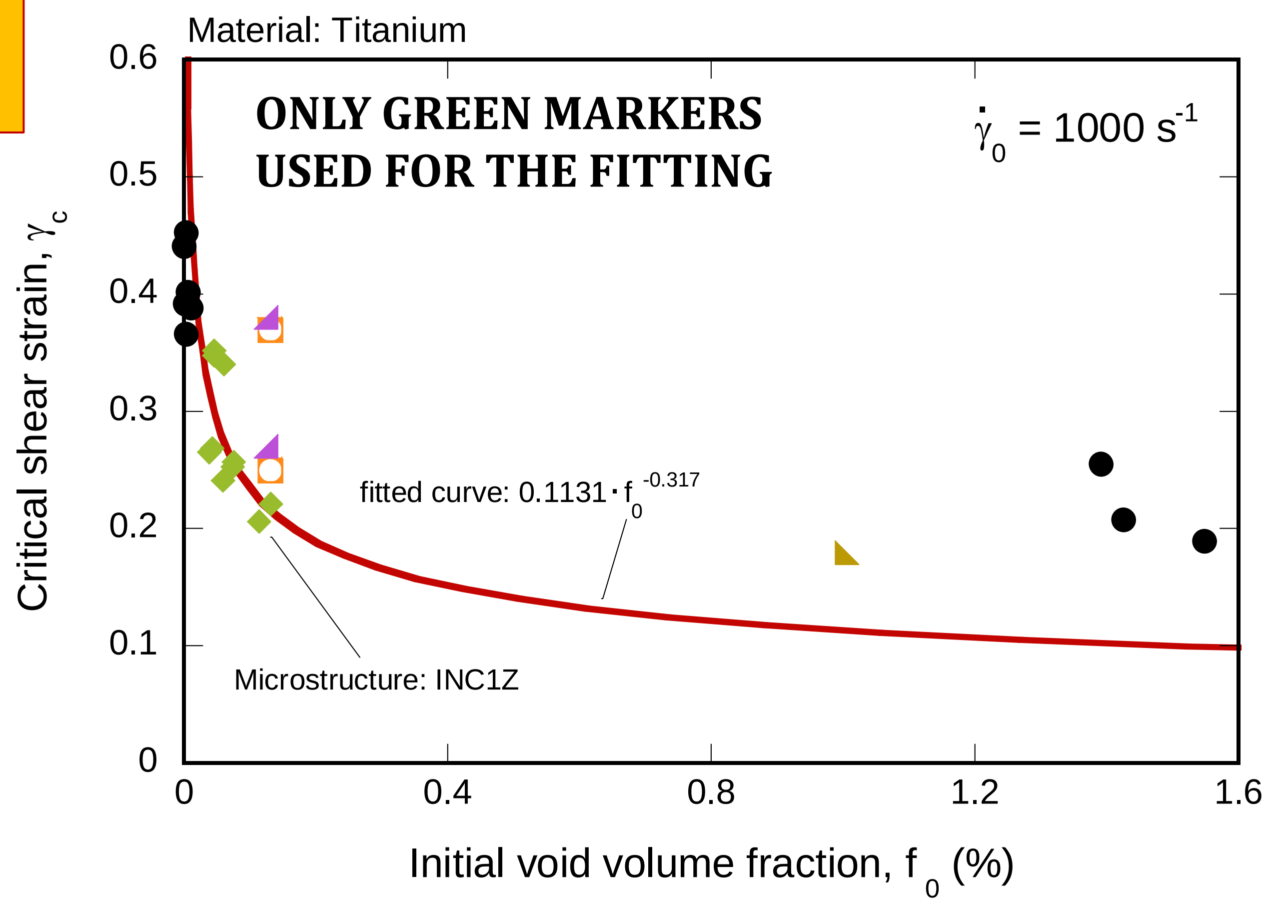

5. Dynamic shear banding: torsion

The effect of porous microstructure

The loss of load carrying capacity depends on the porous microstructure

THE EFFECT OF THE MAXIMUM VOID DIAMETER

KEY MICROSTRUCTURAL FEATURE: VERY GOOD MATCHING

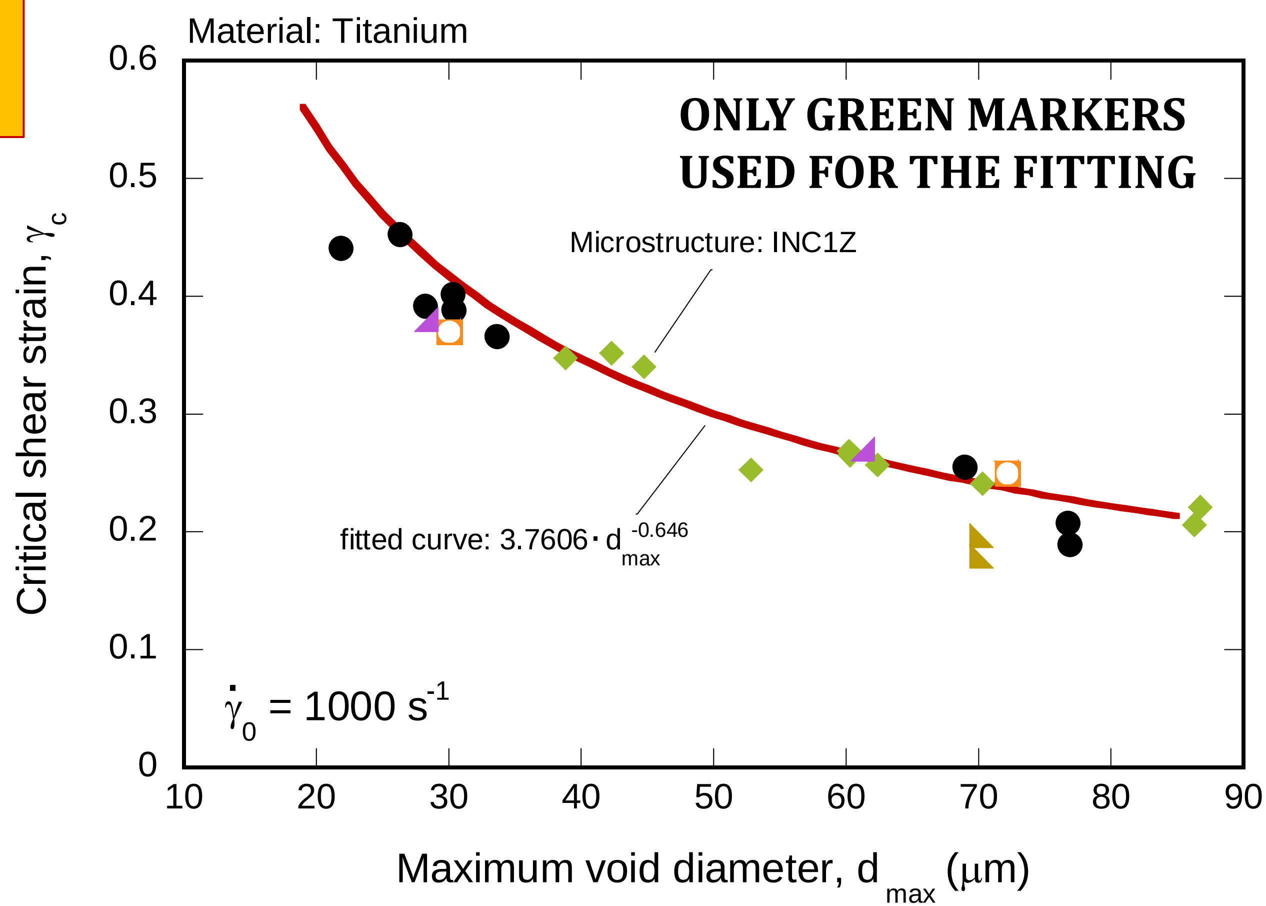

5. Dynamic shear banding: torsion

The effect of porous microstructure

Additional insights: THE MEAN VOIDS SIZE

The void volume fraction is constant

Less but greater voids

Material: Titanium

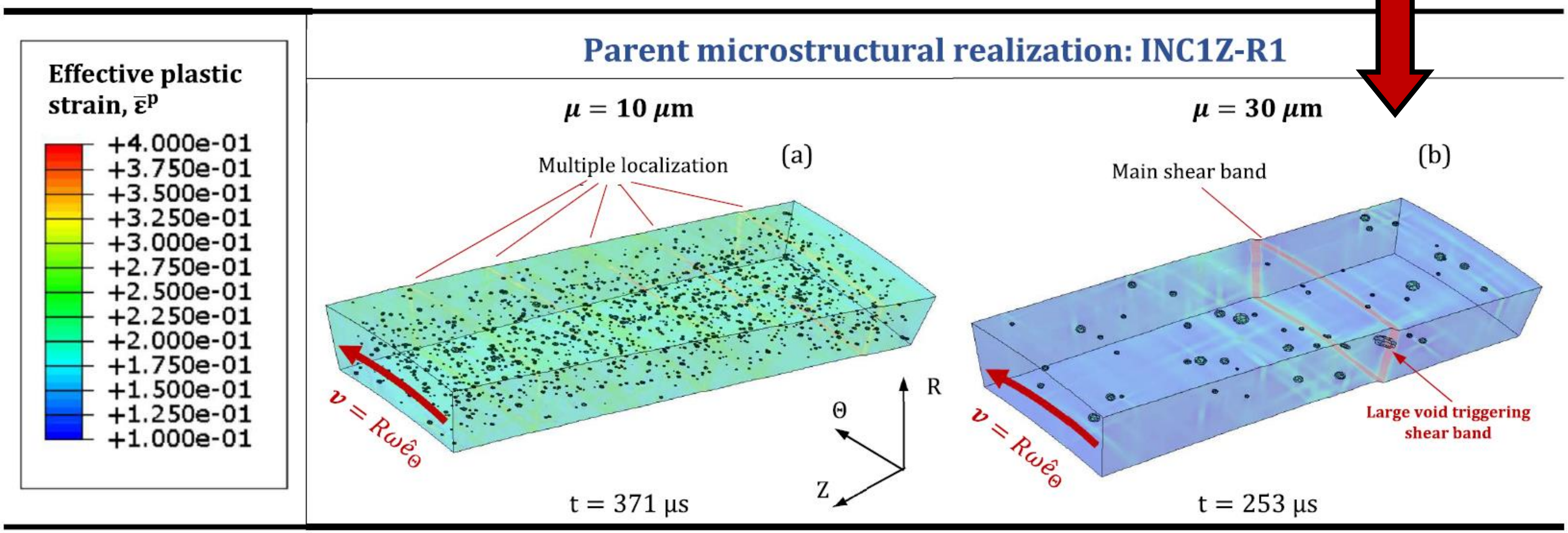

5. Dynamic shear banding: torsion

The effect of porous microstructure

Additional insights: THE MEAN VOIDS SIZE

The void volume fraction is constant

INCREASING THE VOIDS SIZE LEADS TO EARLY LOSS OF LOAD CARRYING CAPACITY

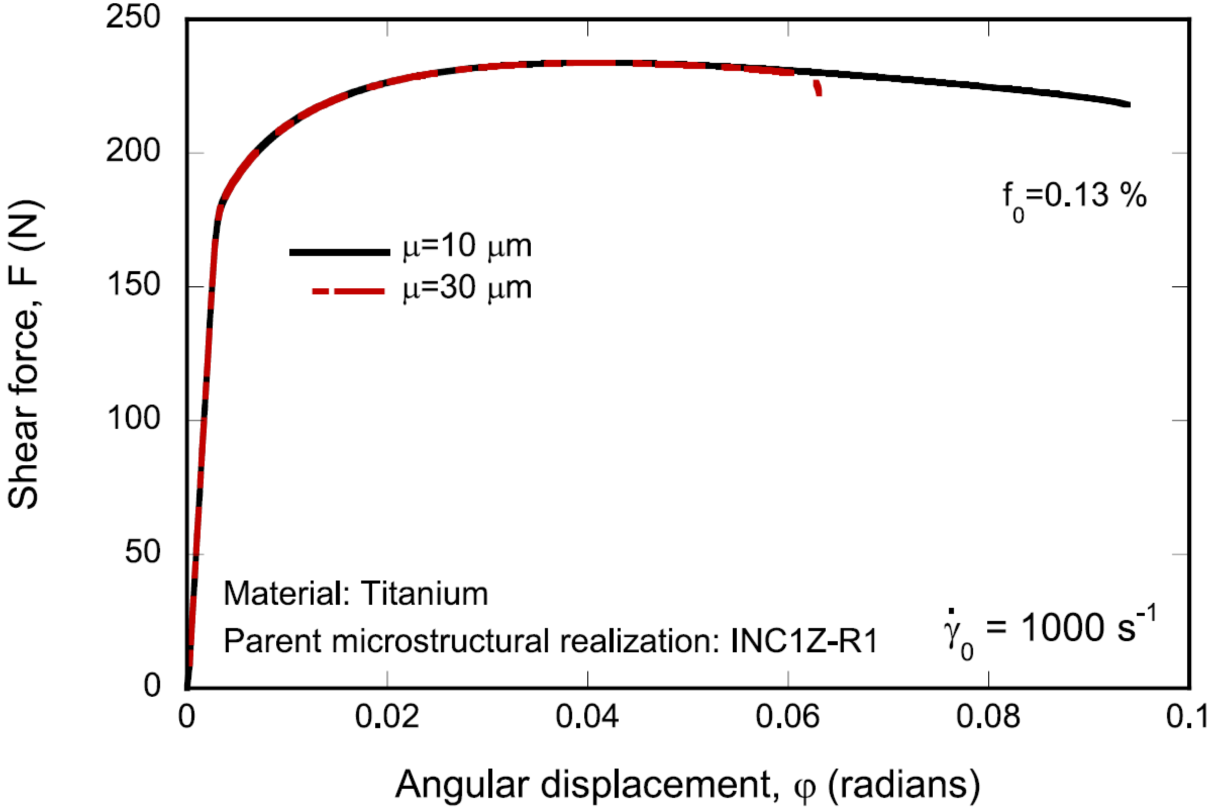

5. Dynamic shear banding: torsion

Dynamic twisting of thin-walled tube

*The **spatial distribution of voids** affects the morphology of the shear localization pattern, as the main shear band is generally nucleated at the location of the largest pore of the microstructure*

*The **size distribution of voids** affects the morphology of the shear localization pattern such that when the pores show large differences in size, the main shear band stands out over the secondary localizations*

*The **maximum voids size** is the main feature of the porous microstructure affecting the specimen ductility, over and above the void volume fraction*

SUMMARY

1. **Introduction**
2. **Objective and methodology**
3. **Porosity distribution**
4. **Dynamic necking: formability**
5. **Dynamic shear banding: torsion**
6. **Conclusions**

SUMMARY

1. Introduction
2. Objective and methodology
3. Porosity distribution
4. Dynamic necking: formability
5. Dynamic shear banding: torsion
6. **Conclusions**

6. Conclusions

Main outcomes

Lay the groundwork of a microstructurally-informed finite element strategy to describe dynamic localization and fracture of porous materials

6. Conclusions

Some limitations

We still lack of a COMPRENHENSIVE EXPERIMENTAL VALIDATION within a wide range of strain rates and material behaviours

The computational time is …. LARGE!

6. Conclusions

Related publications

Vishnu A. R., Marvi-Mashhadi M., Nieto-Fuentes J. C., Rodríguez-Martínez J. A. *New insights into the role of porous microstructure on dynamic shear localization*. International Journal of Plasticity. 2022; 148: 103150

Marvi-Mashhadi M., Vaz-Romero A., Sket F., Rodríguez-Martínez J. A. *Finite element analysis to determine the role of porosity in dynamic localization and fragmentation: Application to porous microstructures obtained from additively manufactured materials*. International Journal of Plasticity. 2021, 143, 102999

6. Conclusions

Related publications

Vishnu A. R., Nieto-Fuentes J. C., Rodríguez-Martínez J. A. *Shear band formation in porous thin-walled tubes subjected to dynamic torsion*. Submitted for publication.

Nieto-Fuentes J. C., Jacques N., Marvi-Mashhadi M., N'souglo K. E., Rodríguez-Martínez J. A. *Modeling dynamic formability of porous ductile sheets subjected to biaxial stretching: Actual porosity versus homogenized porosity*. Submitted for publication.

Nonlinear Solid Mechanics Group

https://www.nonsolmecgroup.com/

The effect of actual porous microstructure on the formation of dynamic necks and adiabatic shear bands

Universidad Carlos III de Madrid

J. A. Rodríguez-Martínez

6. Dynamic shear banding: thick-walled cylinder collapse

Dynamic compression of thick-walled tube

Representative Volume Element: external pressure loading

Fine mesh to capture the shape of the voids

Large computational cost

Eulerian approach for description of the voids collapse

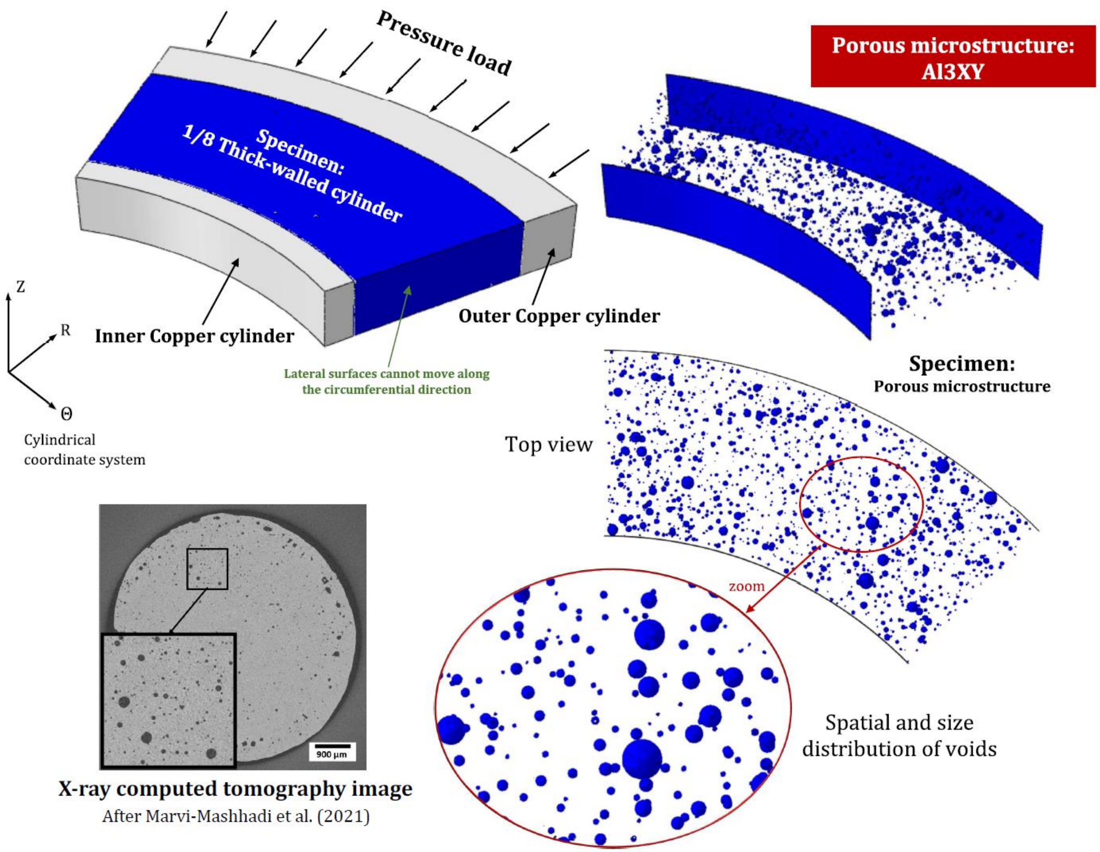

X-ray computed tomography image
After Marvi-Mashhadi et al. (2021)

4. Dynamic necking: formability

Mechanical behavior of the material

Linear elasticity and isotropic von Mises plasticity

Yield stress evolution

$$\sigma_Y = \sigma_0 + \sigma_K \left(\bar{\varepsilon}^p\right)^n \left(\frac{\dot{\bar{\varepsilon}}^p}{\dot{\varepsilon}_{ref}}\right)^m \left(\frac{T}{T_{ref}}\right)^{-\mu}$$

Adiabatic conditions of deformation

$$\dot{T} = \beta \frac{\bar{\sigma}\dot{\bar{\varepsilon}}^p}{\rho C_p}$$

Symbol	Property and units	Value
ρ_0	Initial density (kg/m^3)	7740
C_p	Specific heat (J/kg K)	460
E	Young modulus (GPa)	200
ν	Poisson's ratio	0.3
σ_0	Initial yield stress (MPa)	175.67
σ_K	Hardening modulus (MPa)	530.13
n	Strain hardening exponent	0.167
m	Strain rate sensitivity exponent	0.0118
$\dot{\varepsilon}_{ref}$	Reference strain rate (s^{-1})	0.01
μ	Temperature sensitivity exponent	0.51
T_{ref}	Reference temperature (K^{-1})	300
β	Taylor-Quinney coefficient	0.9

WE DO NOT CONSIDER THE SPECIFIC MECHANICAL BEHAVIOUR OF THE PRINTED METALS WHICH ARE ONLY USED TO OBTAIN POROUS MICROSTRUCTURES

6. Dynamic shear banding: thick-walled cylinder collapse

Onset and development of MULTIPLE shear bands

Evolution of the porous microstructure

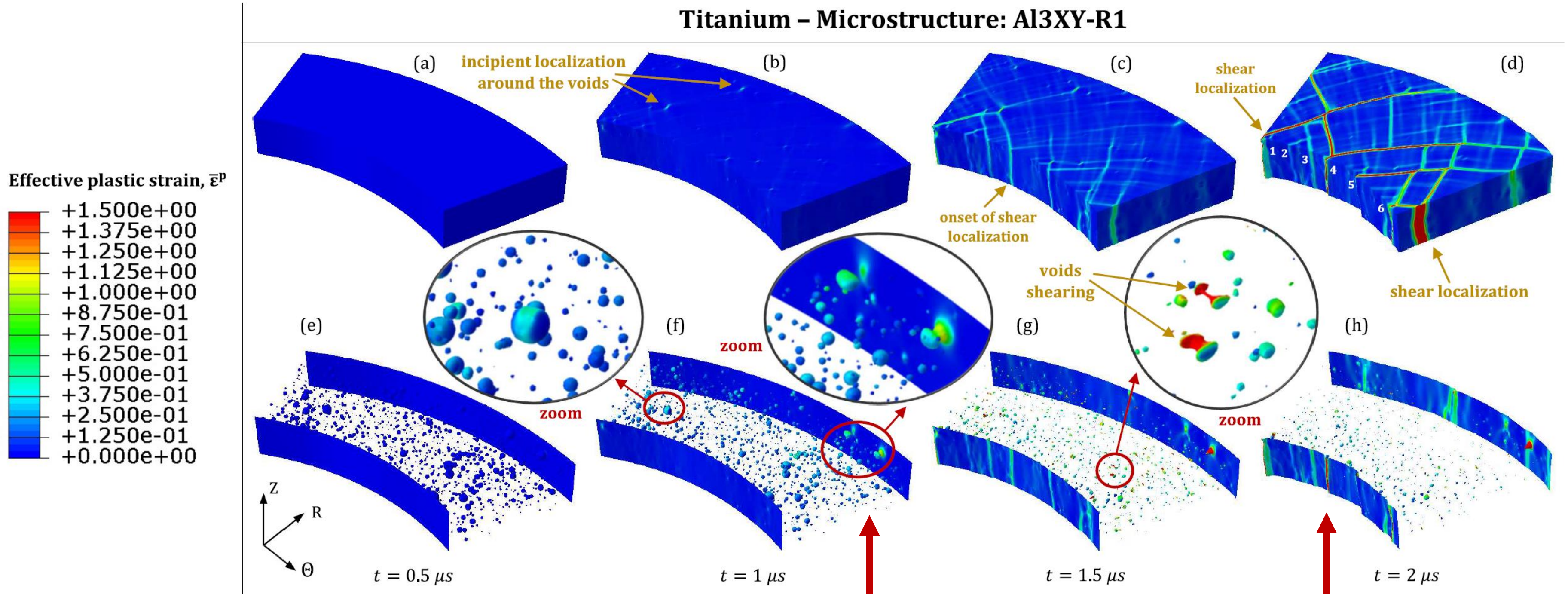

Voids shearing

Voids collapse

6. Dynamic shear banding: thick-walled cylinder collapse

Onset and development of MULTIPLE shear bands

Comparison with fully dense material

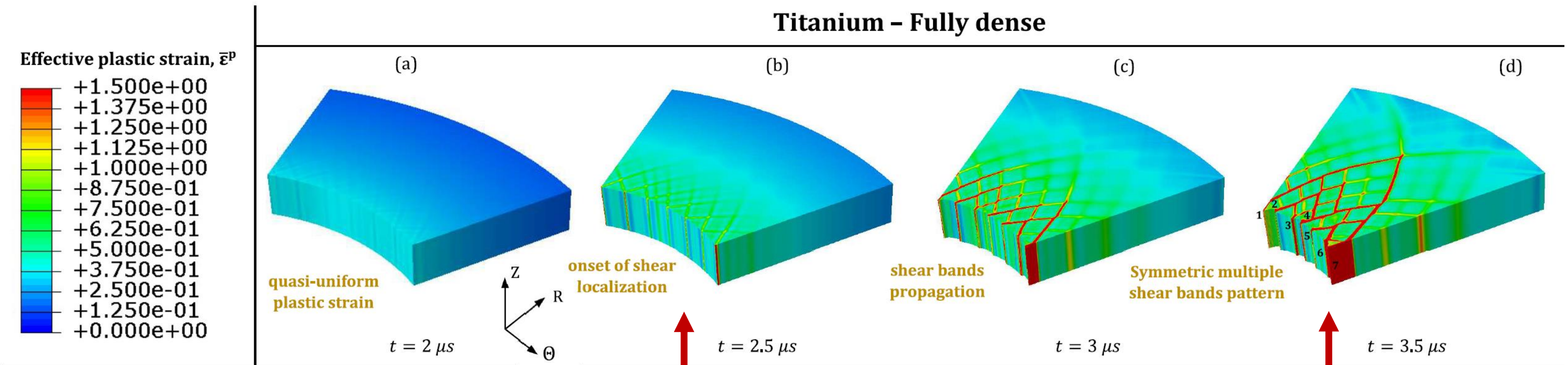

Localization delayed

Symmetric shear band pattern

6. Dynamic shear banding: thick-walled cylinder collapse

The effect of thermal softening

The porous microstructure ALONE does not trigger the localization (the same for the torsion of thin-walled tubes)

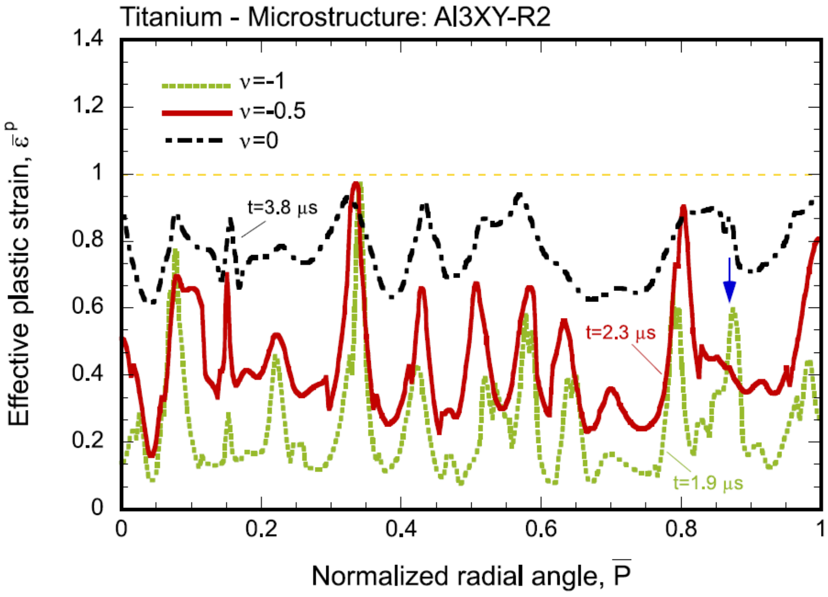

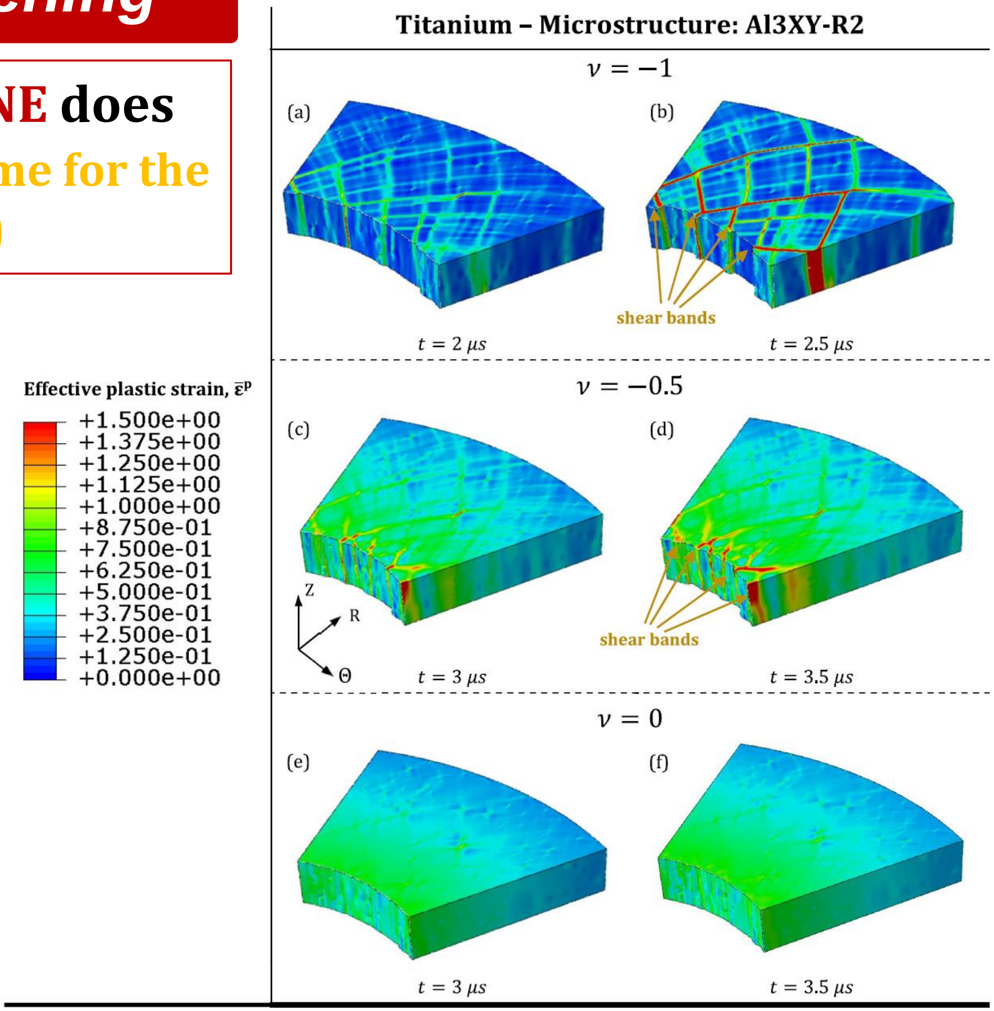

6. Dynamic shear banding: thick-walled cylinder collapse

The effect of porous microstructure

Additional insights: THE MEAN VOIDS SIZE

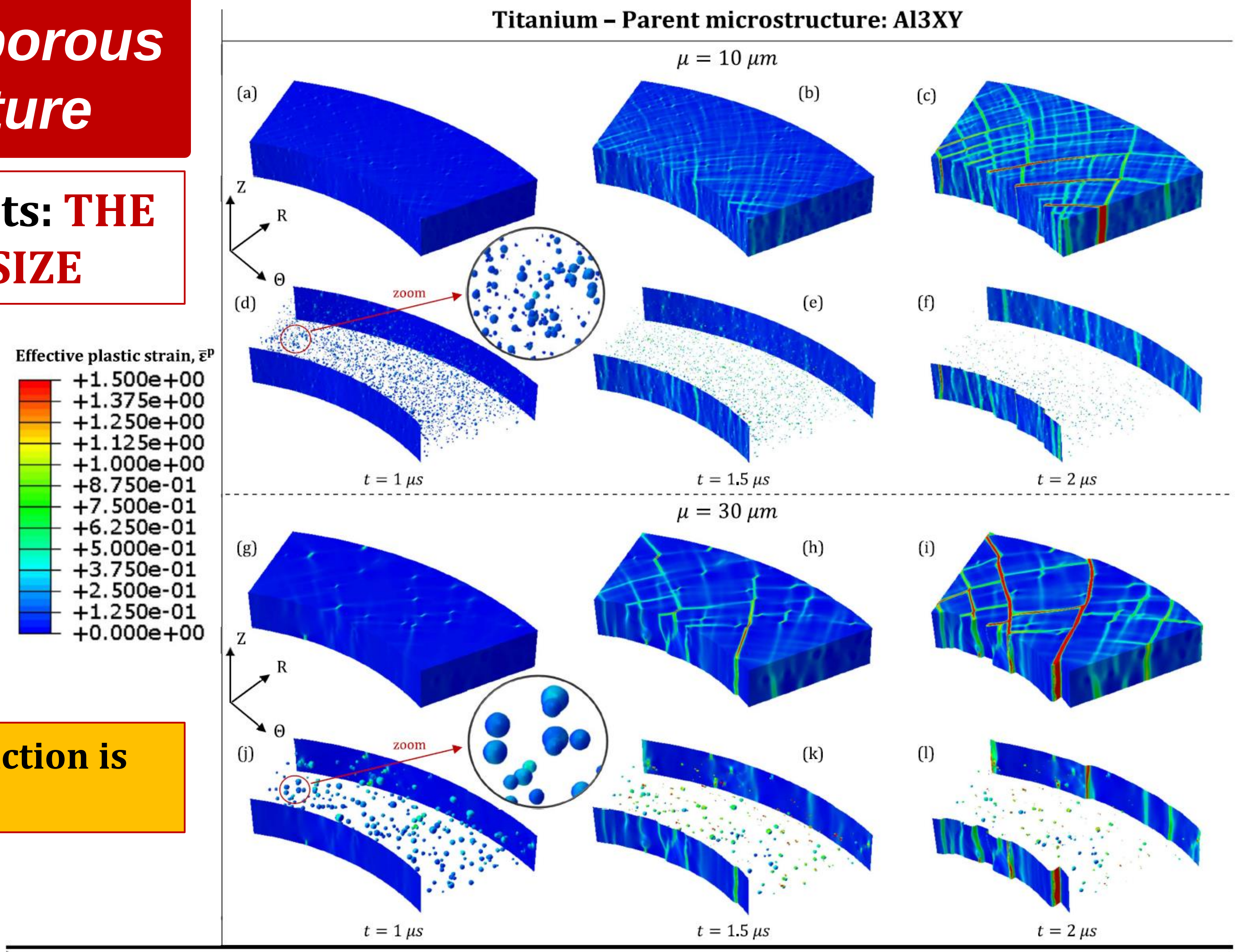

The void volume fraction is constant

6. Dynamic shear banding: thick-walled cylinder collapse

The effect of porous microstructure

Additional insights: THE MEAN VOIDS SIZE

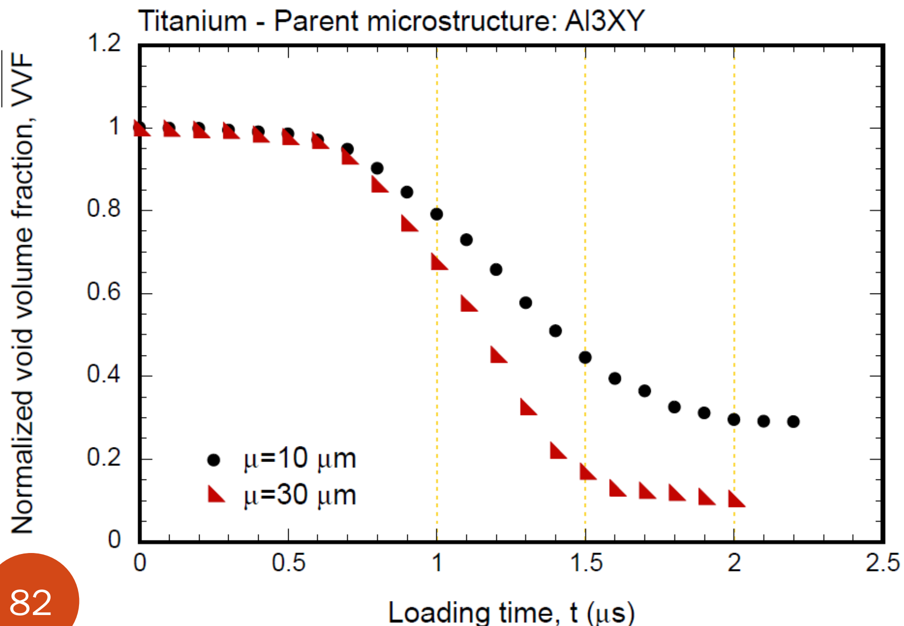

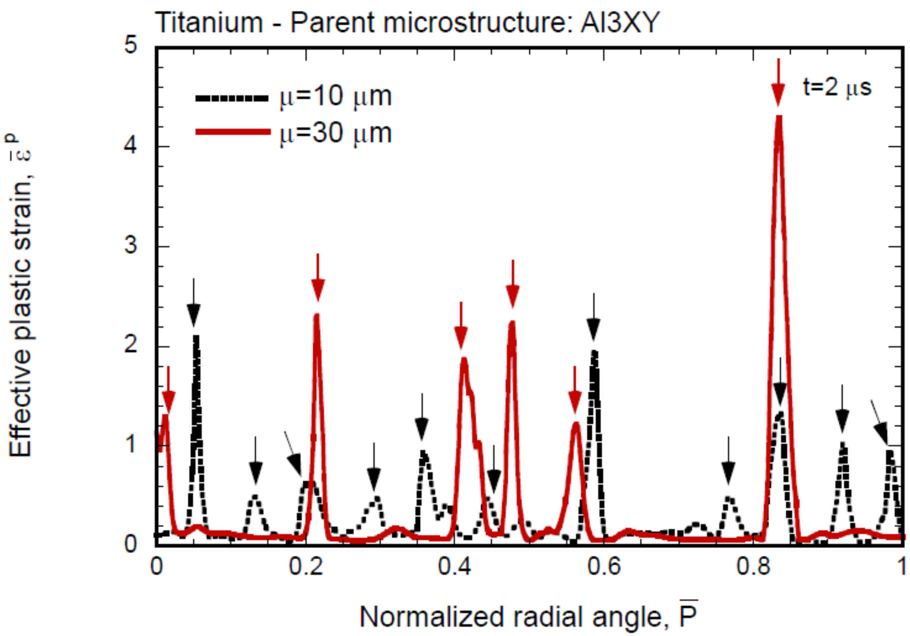

Increasing the voids size favors early shear localization

Increasing the voids size favors early voids collapse

6. Dynamic shear banding: thick-walled cylinder collapse

Dynamic compression of thick-walled tube

***Microstructural porosity** favors the formation and development of shear bands in temperature softening materials*

For temperature independent materials,** microstructural porosity alone **does not trigger the formation of shear bands

*Increasing the **maximum diameter of the voids** favors early shear localization and decreases the number of shear bands*

SUMMARY

1. **Introduction**
2. **Objective and methodology**
3. **Porosity distribution**
4. **Dynamic necking: formability**
5. **Dynamic shear banding: torsion**
6. **Dynamic shear banding: thick-walled cylinder collapse**
7. **Conclusions**

SUMMARY

1. Introduction
2. Objective and methodology
3. Porosity distribution
4. Dynamic necking: formability
5. Dynamic shear banding: torsion
6. Dynamic shear banding: thick-walled cylinder collapse
7. **Conclusions**

8. Plastic shock waves

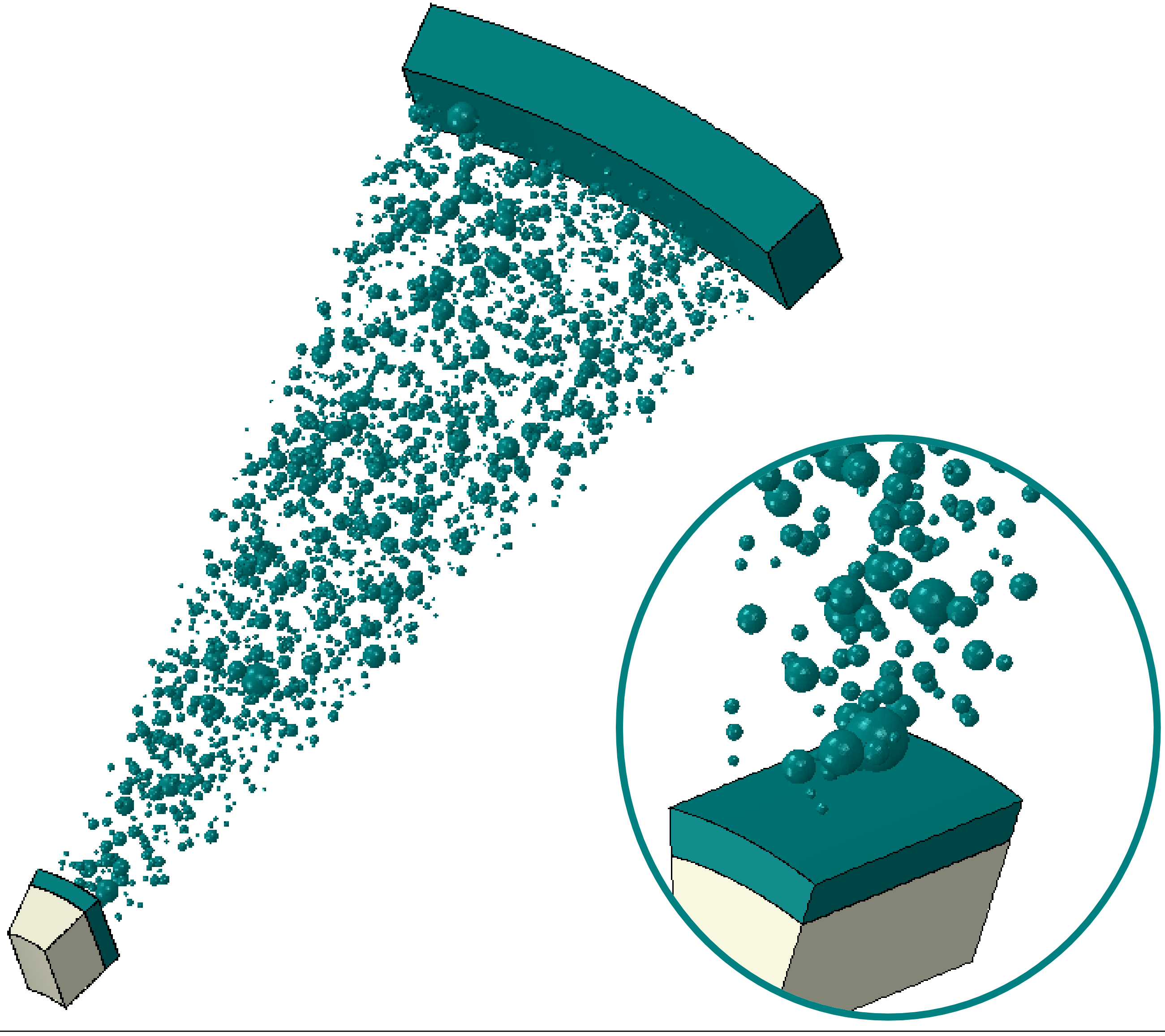

8. Plastic shock waves

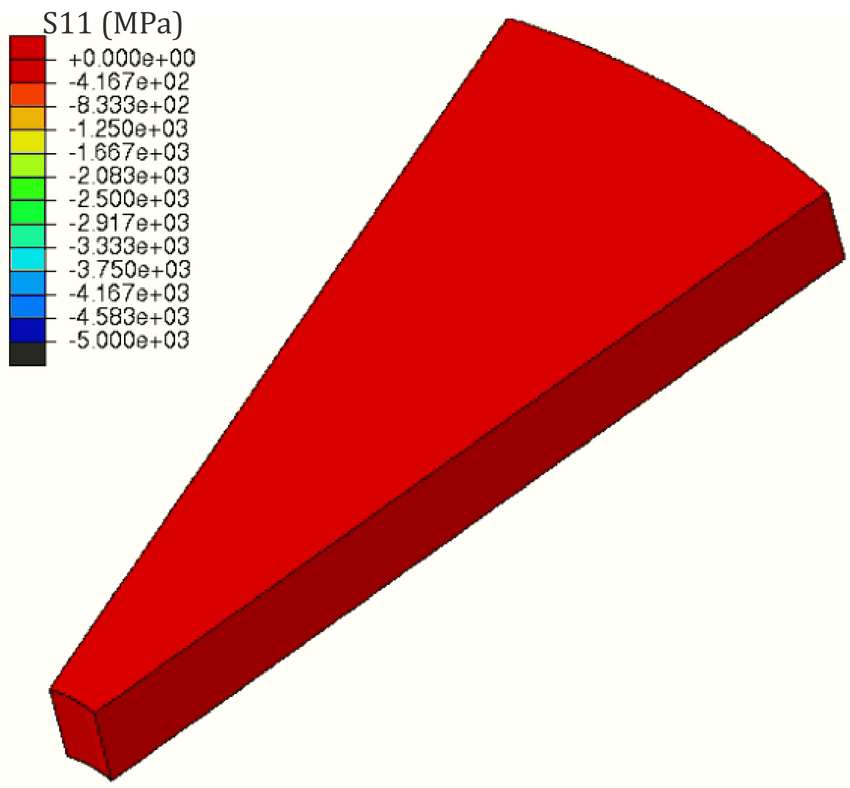

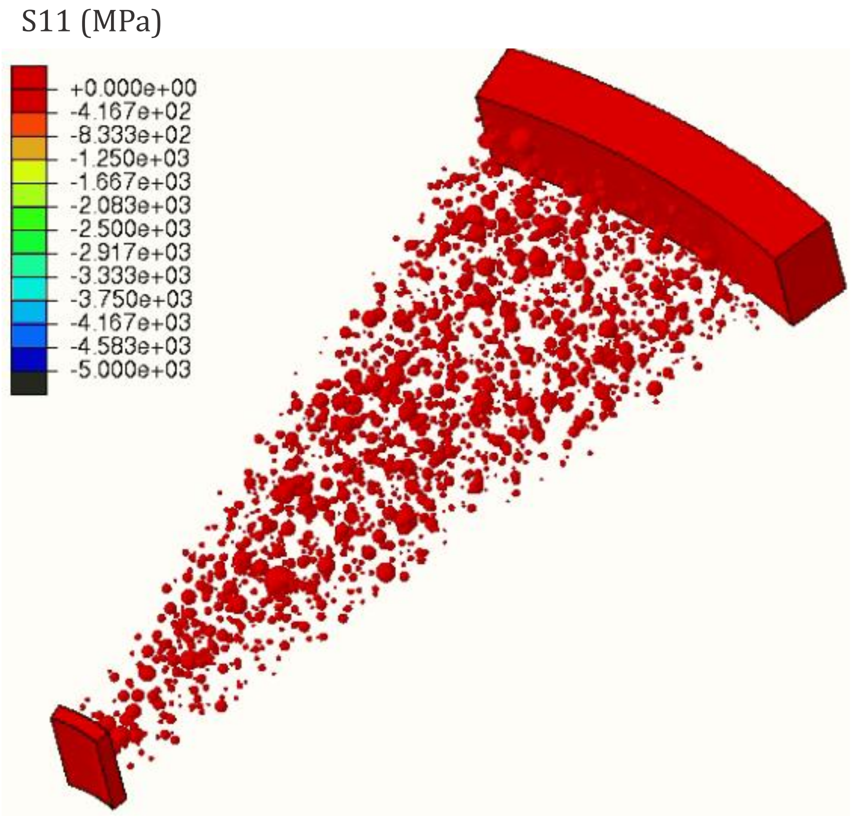

8. Plastic shock waves

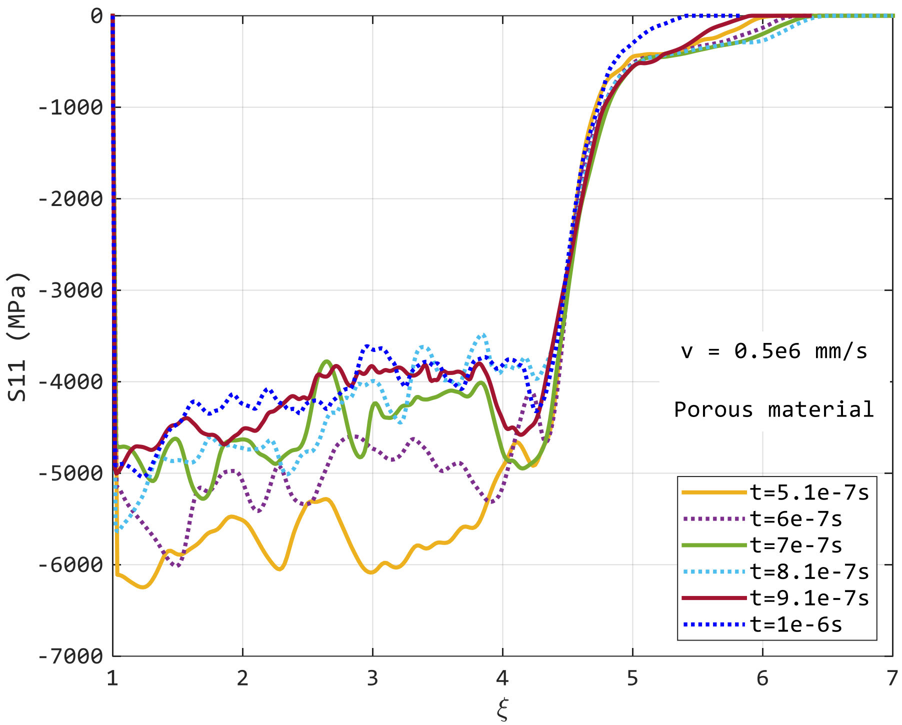

S11 (MPa)

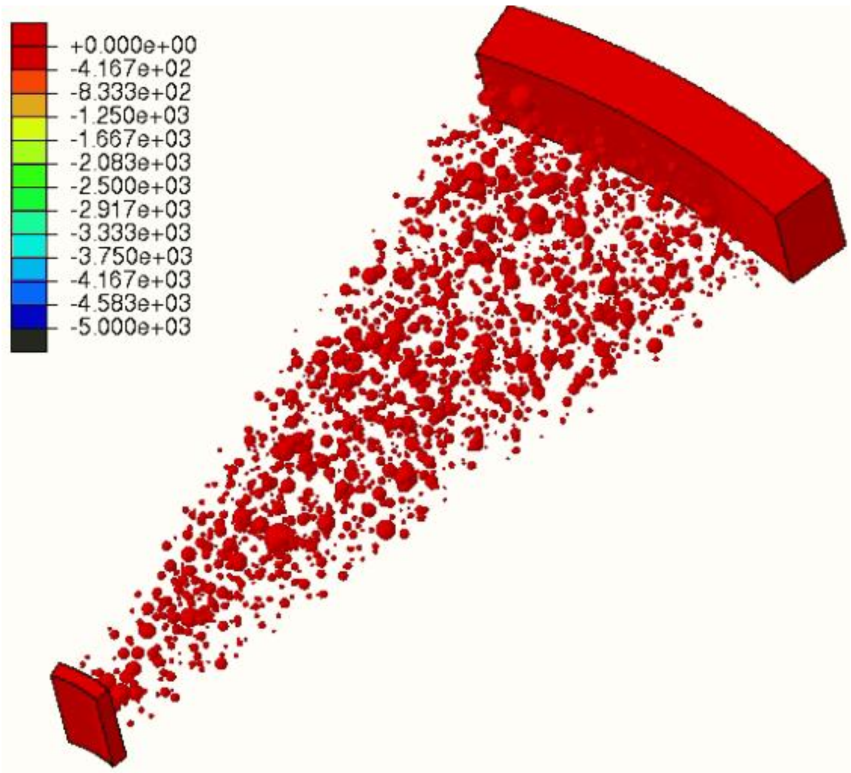

9. Ring expansion

Ring expansion finite element model with

actual distribution of porosity

Inner and outer radii $R_{in} = 15\ mm$ and $R_{out} = 15.5\ mm$

Constant radial velocity V_r varying between 50 and 500 m/s

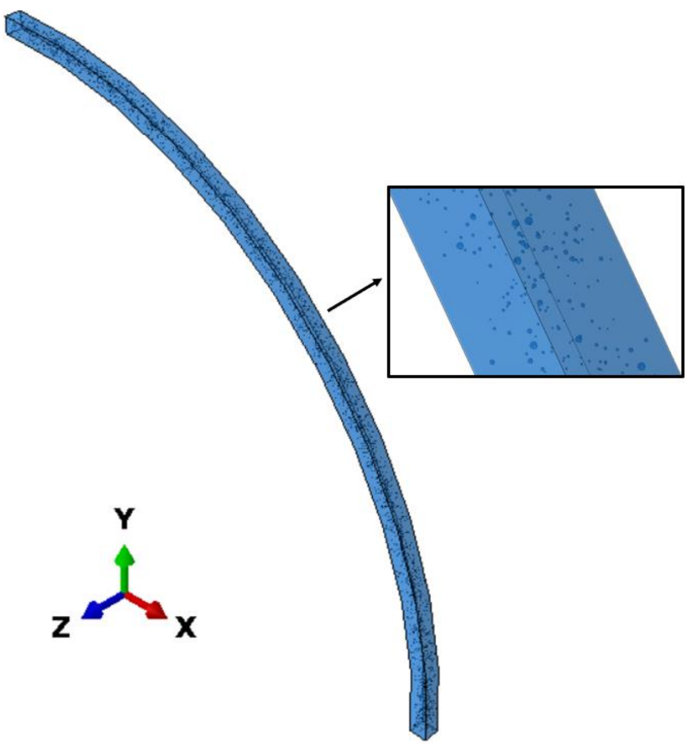

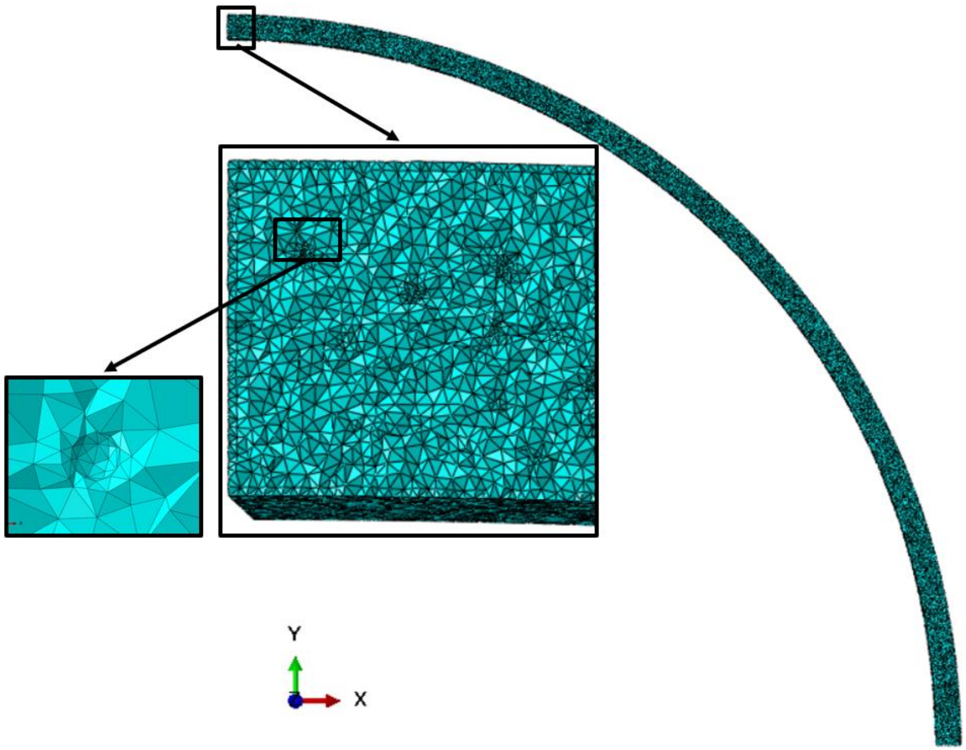

9. Ring expansion

THE INFLUENCE OF MICROSTRUCTURAL REALIZATION IN THE NECKING AND FRAGMENTATION PROCESSES

Statistical approach: distribution of fragment sizes due to variation in fracture strains (Mott 1947, Grady and Olsen (2003), Zhang and Ravi-Chandar (2006, 2008))

SOME NECKS DEVELOP INTO FRACTURES AND SOME NECKS ARE ARRESTED

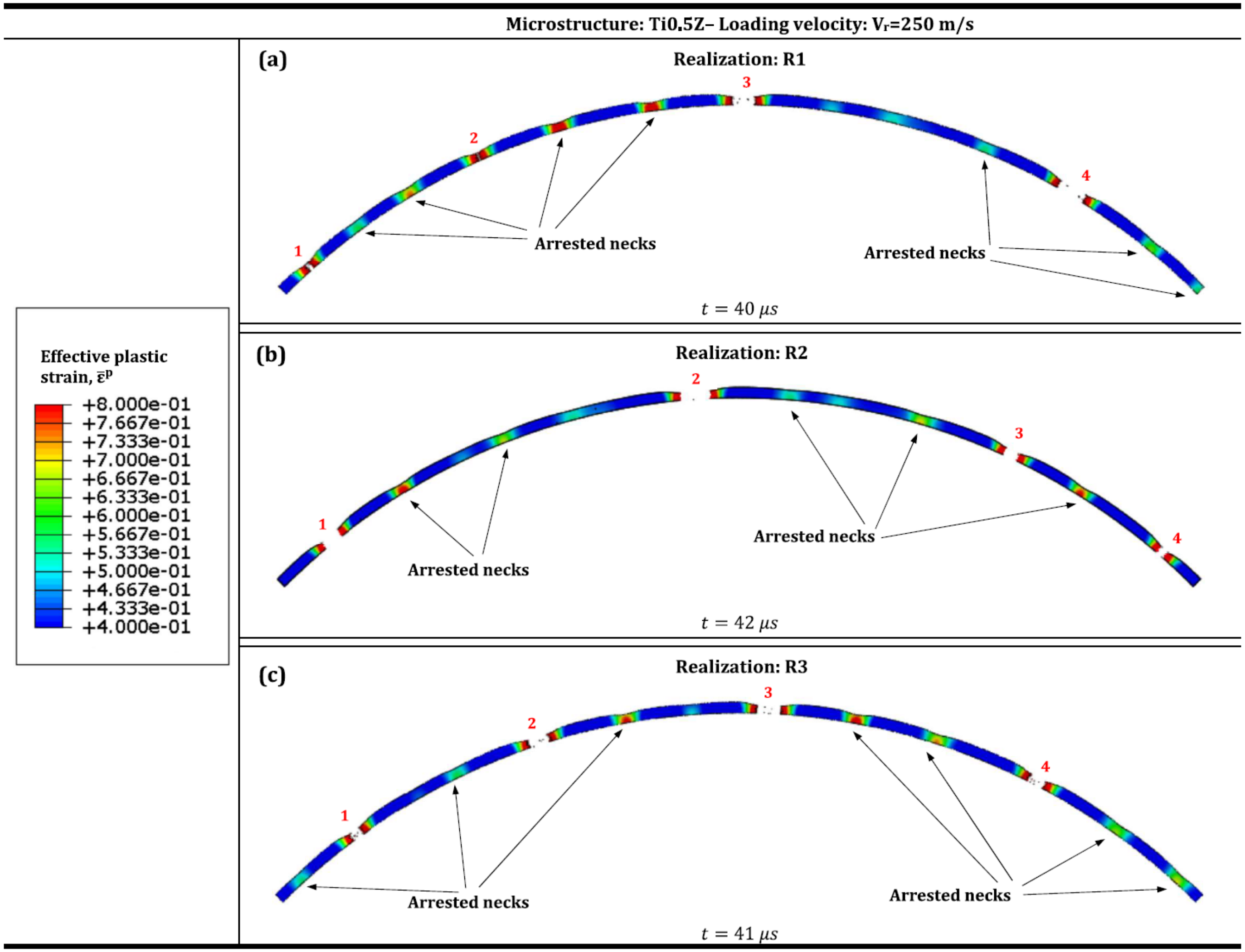

9. Ring expansion

THE INFLUENCE OF LOADING VELOCITY IN THE NECKING AND FRAGMENTATION PROCESSES

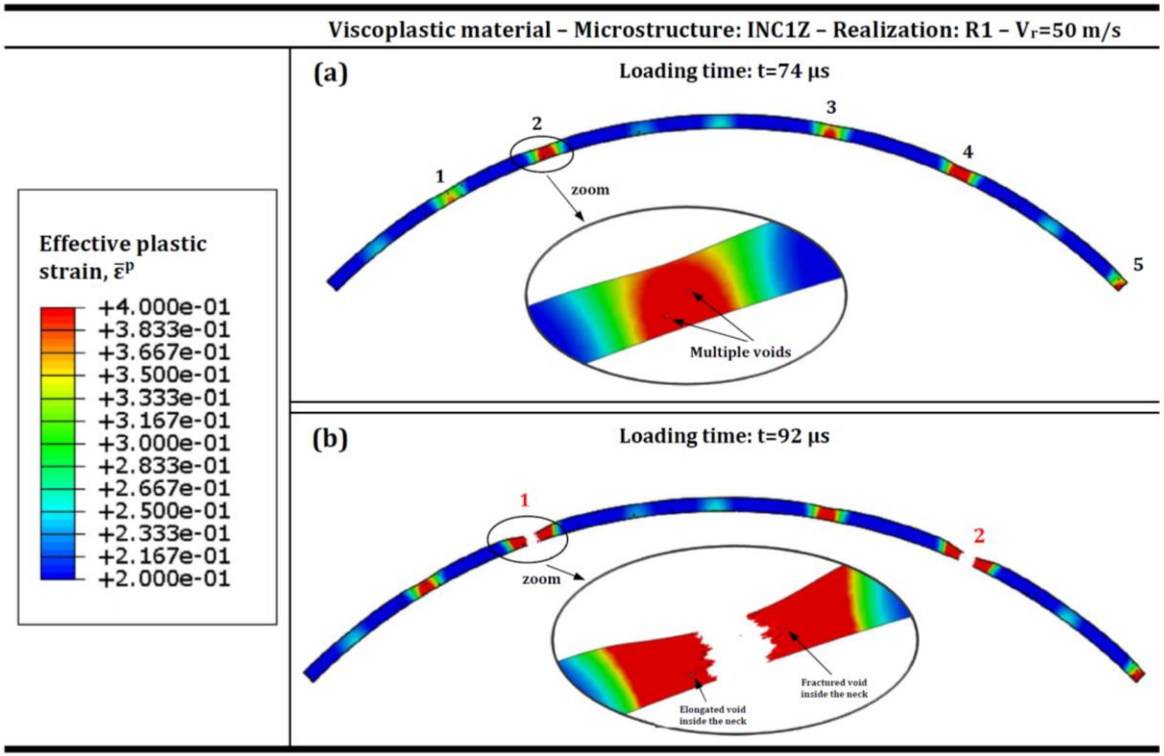

INCREASING VELOCITY INCREASES THE NUMBER OF NECKS AND FRAGMENTS

Deterministic approach: inertia promotes the development of necking wavelengths which are smaller and more dominant as the strain rate increases

9. Ring expansion

THE INFLUENCE OF LOADING VELOCITY IN THE NECKING AND FRAGMENTATION PROCESSES

Deterministic approach: inertia promotes the development of necking wavelengths which are smaller and more dominant as the strain rate increases

INCREASING VELOCITY INCREASES THE NUMBER OF NECKS AND FRAGMENTS

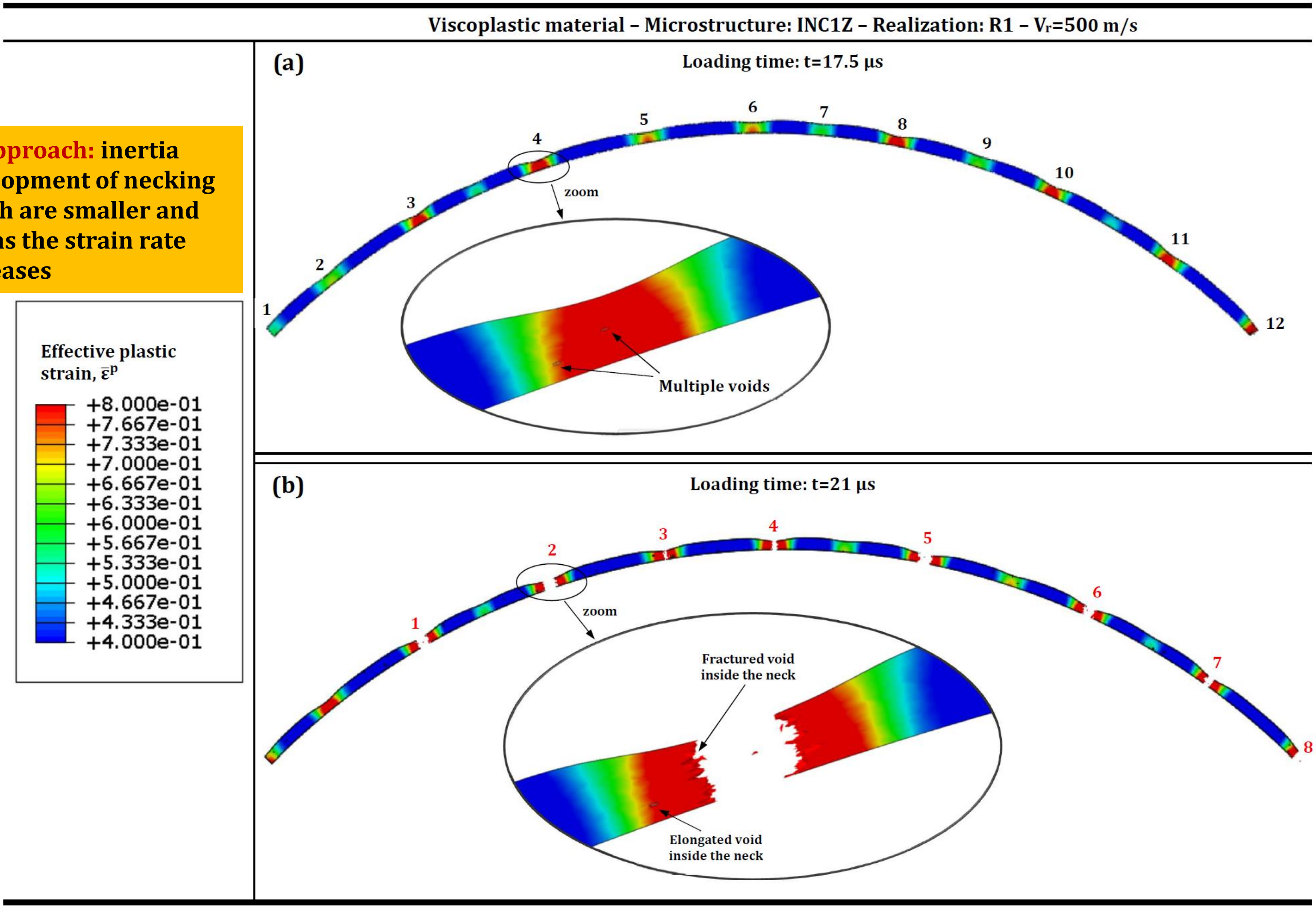

9. Ring expansion

THE INFLUENCE OF LOADING VELOCITY IN THE NECKING AND FRAGMENTATION PROCESSES

Deterministic approach: inertia promotes the development of necking wavelengths which are smaller and more dominant as the strain rate increases

COMPARISON WITH EXPERIMENTS